Cell Reports

Article

CA2/3-dependent stability of frontal mnemonic representations predict episodic deficits in human amnesia

Graphical abstract

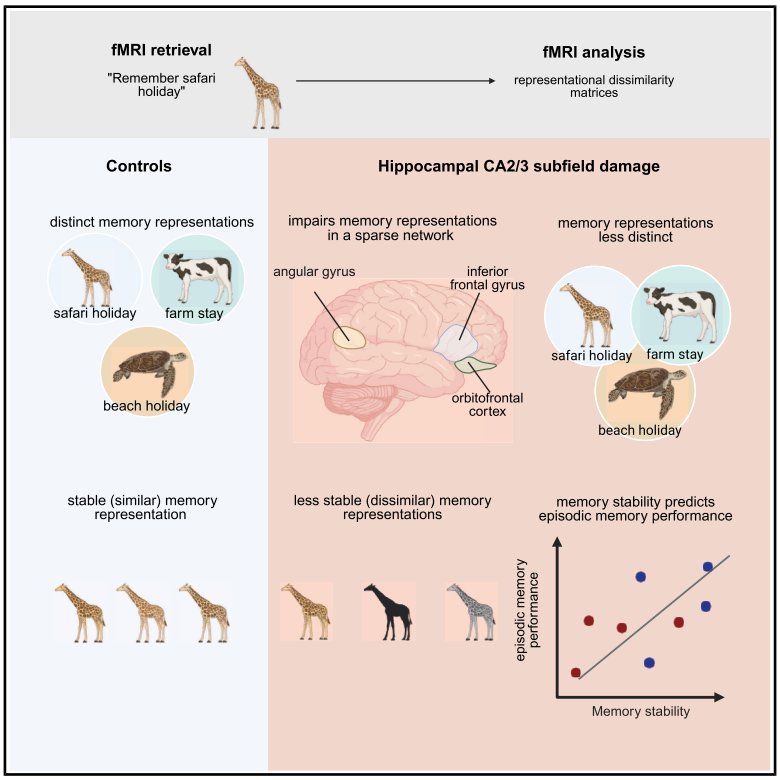

Highlights

- CA2/3 damage impairs generalized episodic memory retrieval in the left angular gyrus
- CA2/3 damage impairs right inferior frontal gyrus (rIFG) distinct mnemonic representations
- CA2/3 damage reduces mnemonic stability in rIFG, rOFC, and rANG
- rIFG and rOFC trial-by-trial stability predicts memory performance

Authors

Thomas D. Miller, Alice L. Hickling, Yan I. Wu, ..., Michael S. Zandi, Eleanor A. Maguire, Clive R. Rosenthal

Correspondence

t.d.miller@ucl.ac.uk (T.D.M.), clive.rosenthal@clneuro.ox.ac.uk (C.R.R.)

In brief

Miller et al. use fMRI to demonstrate that human hippocampal CA2/3 subfield damage results in retrograde autobiographical amnesia and destabilized frontal autobiographical mnemonic representations. Mnemonic stability in the right inferior frontal gyrus predicts retrograde episodic memory performance.

Miller et al., 2025, Cell Reports *44*, 116527
November 25, 2025
https://doi.org/10.1016/j.celrep.2025.116527

CellPress

Cell Reports

CellPress
OPEN ACCESS

Article

CA2/3-dependent stability of frontal mnemonic representations predict episodic deficits in human amnesia

Thomas D. Miller,[1,2,12,*] Alice L. Hickling,[1] Yan I. Wu,[1] Joseph H. Zhou,[3] Adam E. Handel,[4,5] Ester Coutinho,[6,7,8] Thomas A. Pollak,[9] Michael S. Zandi,[2] Eleanor A. Maguire,[1,11] and Clive R. Rosenthal[10,11,*]

[1]Department of Imaging Neuroscience, University College London, London, UK
[2]UCL Queen Square Institute of Neurology, National Hospital for Neurology and Neurosurgery, Queen Square, London, UK
[3]UCL Medical School, University College London, London, UK
[4]Oxford Autoimmune Neurology Group, Nuffield Department of Clinical Neurosciences, University of Oxford, Oxford, UK
[5]Department of Neurology, John Radcliffe Hospital, Oxford University Hospitals NHS Foundation Trust, Oxford, UK
[6]Center for Neuroscience and Cell Biology, Universidade de Coimbra (CNC-UC), Coimbra, Portugal
[7]Centre for Innovative Biomedicine and Biotechnology (CiBB), Universidade de Coimbra, Coimbra, Portugal
[8]Católica Medical School, Universidade Católica Portuguesa, Rio de Mouro, Portugal
[9]Department of Psychosis Studies, Institute of Psychiatry, Psychology and Neuroscience, King's College London, London, UK
[10]Nuffield Department of Clinical Neurosciences, University of Oxford, Oxford, UK
[11]These authors contributed equally
[12]Lead contact
*Correspondence: t.d.miller@ucl.ac.uk (T.D.M.), clive.rosenthal@clneuro.ox.ac.uk (C.R.R.)
https://doi.org/10.1016/j.celrep.2025.116527

SUMMARY

The hippocampus reconstructs past experiences by integrating sensory, perceptual, and conceptual information across a cortico-hippocampal autobiographical memory network. Here, in 18 human participants with amnesia, we decode the effects of bilateral focal hippocampal damage on distinct autobiographical representations using representational dissimilarity matrices (RDMs). Hippocampal pathology results in impaired generalized episodic memory retrieval RDM model fit in the left angular gyrus and in reduced distinct episodic memory RDM model fit in the right inferior frontal gyrus (rIFG), while right angular gyrus (rANG) and right orbitofrontal cortex (rOFC) fall below multiple correction thresholds. Trial-by-trial voxel-representational stability is reduced in the rANG, rIFG, and rOFC. The RDM model fits and mnemonic stability are predicted by total CA2/3 volumes. Trial-by-trial retrieval stability within the rOFC and rIFG predicts episodic memory performance, providing a direct neural correlation between hippocampal dysfunction, altered mnemonic representations, and amnesia.

INTRODUCTION

Autobiographical recollection, a fundamental component of episodic memory, involves the reconstruction of past experiences by integrating sensory, perceptual, and conceptual information into cohesive personal narratives.[1–5] This integration relies on a large-scale autobiographical memory network (AMN) involving parietal regions, such as the angular gyrus and the dorsal/ventral parietal cortex, which enable multimodal sensory processing and contextual framing.[5–13] Temporal-frontal interactions, involving the hippocampus and ventromedial and medial prefrontal cortices, facilitate the integration of conceptual elements of recollection, including schema formation, self-processing, and perceptual abstraction.[14–20]

The hippocampus is also essential for forming coherent mental representations required for episodic memory, integrating both unimodal and multimodal inputs from broader processing networks.[1–5,21] Lesion studies underscore the essential role of the hippocampus in retrieving episodic details because hippocampal damage often leads to episodic, and especially autobiographical, amnesia.[22–27] Functional MRI (fMRI) shows that hippocampal damage and wider medial temporal lobe (MTL) pathology disrupt the dynamic interactions between the hippocampus and other AMN regions, which impair connectivity and memory processes needed for autobiographical retrieval.[28–31]

Although prior fMRI human hippocampal lesion studies have been informative, their interpretation is often complicated by the inclusion of individuals with anatomical damage that extends beyond the hippocampus to the other medial temporal lobe structures and associated network nodes.[32–34] The focal models of hippocampal damage in humans are rare,[22,31,35–37] limiting group-level behavioral and fMRI assessments of its impact on autobiographical memory. An additional concern is that prior fMRI studies of participants with hippocampal damage used univariate analyses, thereby failing to capture important details

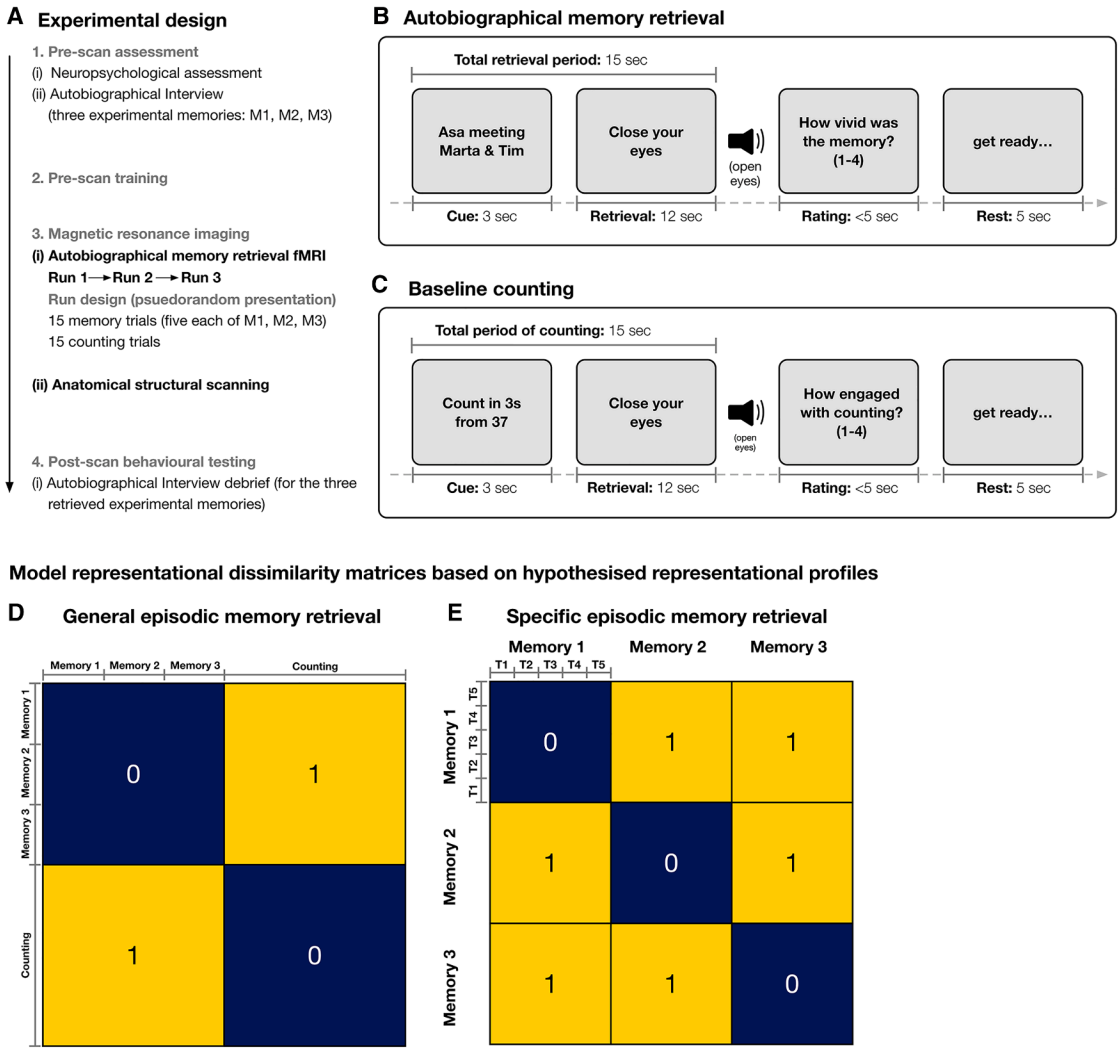

Figure 1. Experimental design. Episodic memory decoding task protocol

(A) The experiment comprised four separate phases. (1) Two weeks prior to the scan date, all participants underwent an extensive neuropsychological assessment and the Autobiographical Interview (AI) procedure to acquire three personal episodic memories that would be retrieved during experimental scanning. On the day of scanning, all participants underwent extensive (2) pre-scan training and (3) intra-scan training (see STAR Methods). Once in the MRI scanner, all participants undertook three fMRI runs comprising two conditions (autobiographical memory retrieval and the baseline counting task). (4) Post-scan behavioral testing. Immediately after the end of two anatomical scans, a final debriefing on the experimental memories was conducted. Participants were asked to recount what they retrieved for each memory during the retrieval periods using the AI procedure. These debriefing interviews were recorded in a digital audio format and then transcribed for offline scoring.

(B) Autobiographical memory retrieval. Participants were presented with a 3-s verbal cue for a specific autobiographical memory. After the offset of the cue, the participants were prompted to close their eyes and retrieve the memory with as much visual and verbal episodic detail as possible. The prompt to "close your eyes" remained on the screen for 12 s while the participants continued to retrieve the cued memory. An auditory instruction to "open your eyes" cued the end of the retrieval period.

(C–E) Counting trials. Participants were presented with a starting number for 3 s and then a specific interval to count up in 3 s, followed by the same "close your eyes" screen prompt for 12 s. After each memory retrieval trial and counting trial, the participants were then asked to rate either "how vivid was the recollection?" or "how engaged were you with the task?" (see STAR Methods), respectively, and indicate their response using an MRI-compatible button box. All trials were followed by a 5-s rest period before the next trial. No inter-trial jitter was used, given the length of the retrieval trials. Immediately after the completion of the fMRI experimental phase, each participant underwent two anatomical scans. Model representational dissimilarity matrices (RDMs) based on hypothesized representational profiles. We performed a model fit analysis by comparing two RDMs within the representational patterns observed in the individual participants' RDMs (D and E). Each specific memory in (D) and (E) is further subdivided into five trials per run (as shown in E), and there were also 15 counting trials per run. Final values were averaged across runs. These matrices were designed to test two key hypotheses: (D) whether focal hippocampal subfield damage resulted in between-group differences in representational content during episodic memory retrieval, as a general process and collapsed across all memory retrieval trials (15 memory trials per run), compared to the control counting task (generalized episodic memory retrieval); and (E) whether focal hippocampal subfield damage impaired the

(legend continued on next page)

about the content and structure of reinstated memories. In contrast, more recent work using multivariate analyses in neurologically intact humans suggests that the hippocampus coordinates the reinstatement of distributed neural patterns associated with an event during its initial encoding period.[38–41] This highlights the need for more sophisticated analyses[12,42–44] in studies of hippocampal amnesia.

Here, we investigated the effects of bilateral focal hippocampal damage, associated with episodic amnesia, across the AMN, decoding how this damage altered the representational content of pre-morbid, recently (~5 years) acquired autobiographical memories during retrieval. Eighteen human participants with amnesia, secondary to a single etiology, leucine-rich glioma-inactivated-1-limbic encephalitis (LGI1-LE),[37,45–47] were recruited and compared with a group of 18 matched control participants (see Figure 1). Anatomical MRI-based characterization confirmed that the damage was bilateral and confined to the hippocampus in all participants with amnesia (bilateral volume loss was confined to CA1 and CA2/3 subfields, mean reductions = −18% and −41%, respectively). These novel results of focal hippocampal damage align with previous findings in the same etiology.[31,37,48–55]

We then used fMRI to compare autobiographical memory retrieval in the participants with hippocampal damage-mediated amnesia with the control group. The retrieval protocol was optimized for decoding representational content. Episodic and semantic details associated with each autobiographical memory retrieved in the scanner were interrogated using an objective, parametric, quantitative method, the Autobiographical Interview (AI) procedure.[56] The AI was chosen because it has demonstrated sensitivity to detecting and characterizing episodic amnesia linked with hippocampal pathology.[24,31,37,57–59] Consistent with prior results,[31,37] we found that autobiographical memories in the group with hippocampal amnesia were associated with a loss of internal (episodic) details of autobiographical memories, but not external (semantic) details. Accordingly, we use the term "episodic," rather than "autobiographical" memory because this better reflects the re-experiential component of autobiographical memories that are specifically impaired after bilateral hippocampal damage.

Unlike previous studies of hippocampal damage that focused on overall univariate activity changes, we measured the consistency (stability) of the neural pattern activity each time a memory was retrieved. Moreover, to decode specific memories, we calculated representational dissimilarity matrices (RDMs) based on memory-specific neural response patterns. RDMs (an approach within multivoxel pattern analysis, MVPA) have been used to characterize voxel-level signal patterns across multiple voxels in response to specific memories, revealing fine-grained representational structures and enabling discrimination between individual memories,[42,60] even when the overall activity levels in a region remain relatively constant.[61,62] Application of MPVA-based pipelines in healthy adults has linked hippocampal activity with the successful differentiation, reinstatement, and retrieval of specific episodic memories.[12,43,44,63–68] When applied to a single case of developmental amnesia, MVPA has revealed reduced pattern similarity between perception and recall phases, despite preserved stimulus-specific brain activity during both encoding and retrieval.[69] Here, we employ RDMs during retrieval to decode representational content to quantify the stability and distinctiveness of autobiographical memories in focal hippocampal amnesia. In the current study, RDMs offered two advantages over other frameworks within MVPA[70]: (1) we obtained quantitative measures of dissimilarities to compare the neural data with different experimental hypotheses about the type of information being represented in a brain region during mnemonic retrieval[14,42,61,71,72] and (2) we were able to quantify the consistency of voxel activity patterns across multiple stimulus presentations, yielding a measure that indicated the stability of specific personal event memories.[14,70–72]

Hippocampal damage is also known to impair the differentiation of memories,[73–77] which aligns with findings from healthy adults that have identified the hippocampus, especially the dentate gyrus and CA3 subfields, with unique and discriminable activity patterns for similar stimuli (such as memories).[78] Together, these observations lead to the hypothesis that a loss of pattern separation, and hence mnemonic discriminability, may partially explain episodic memory deficits following hippocampal damage. To investigate how hippocampal damage affects the differentiation of episodic memories, we thus tested whether RDMs would show reduced discriminability (or distinctiveness)[70] between episodic memories in the group with hippocampal amnesia compared to healthy controls. Specifically, we predicted decreased dissimilarity between neural representations of these episodic memories for the group with hippocampal amnesia. Our second hypothesis was that these effects would be most pronounced in AMN regions that are closely connected to the hippocampus, given that lesions involving network hubs like the hippocampus can disrupt functional connectivity of local and non-local brain regions.[31,79–82] Our third hypothesis was that RDM-derived neural measures in affected AMN nodes would predict the amount of episodic detail remembered on the basis that differentiated neural representations enhance richly detailed remembering and reduce interference from similar memories.[38,83,84] This aligns with evidence that RDM-derived neural measures can serve as a neural code informing behavioral responses.[31,37,64,85–87] Our fourth hypothesis was that the extent of hippocampal pathology would be linked to representational stability, with greater damage leading to less stable representations, evidenced by higher dissimilarity across trials for the same memory and/or more similarity across different memories.[70] Such instability in the group with hippocampal amnesia would suggest a less consistent representational structure, signaling degraded memory retrieval.[70] Our study, therefore, sought to

ability to represent specific episodic memories (specific episodic memory retrieval). Each memory cell contains five trials per run of that specific memory (denoted as Trial [T]1, T2, T3, T4, and T5). Each of the 30 trials (15 memory and 15 counting) per run was then subjected to trial-by-trial correlation analyses. Counting trials are not shown in (B) for simplicity. Model matrices were constructed to feature a value of 1 in hypothesized high-dissimilarity cells and a value of 0 in hypothesized low-dissimilarity cells.

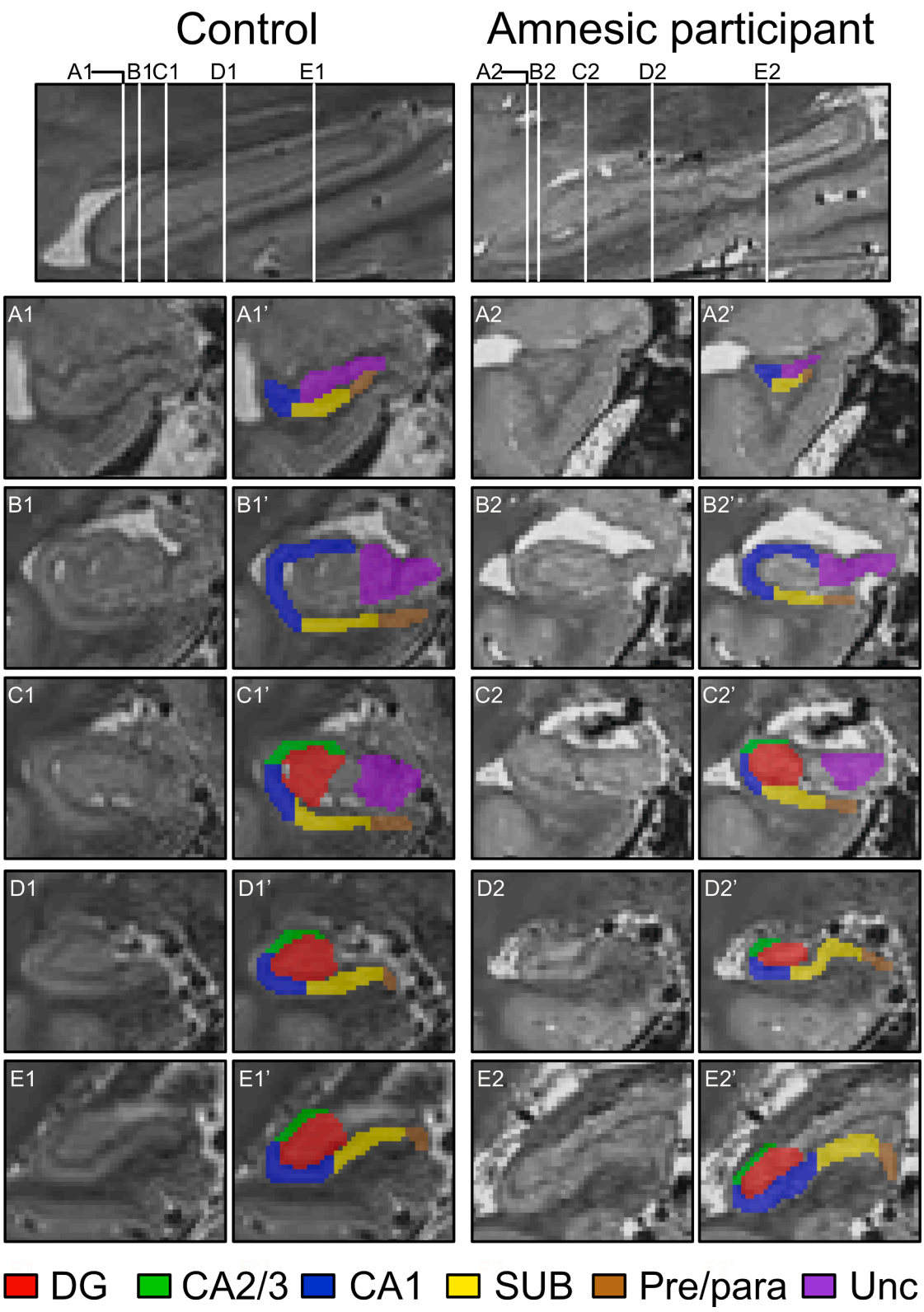

(legend on next page)

provide new insight into how hippocampal dysfunction is expressed in the neural systems that support autobiographical memory.

RESULTS

First, we report the results of structural brain imaging analyses that were designed to determine whether the damage was limited to the hippocampus and to establish which hippocampal subfields were damaged in the group with hippocampal amnesia. Second, we report episodic and semantic memory retrieval performance in the group with hippocampal amnesia, using the degree of hippocampal subfield loss to predict the severity of retrograde episodic amnesia.[31,37] Third, we report the results from fMRI RDM analyses designed to determine whether neural response model fit in the AMN differed in the group with hippocampal amnesia and controls for measures of general episodic memory and specific episodic memories. Fourth, we report the stability of specific memories using the averaged dissimilarity scores from the first-level RDM analysis (calculated as 1: Fisher-transformed Pearson correlation score), and how these stability measures relate to the degree of hippocampal subfield damage and episodic memory performance.

Selective bilateral hippocampal subfield volume loss

The group with hippocampal amnesia exhibited focal hippocampal subfield pathology in the CA2/3 and CA1 subfields, according to quantitative three-dimensional whole-hippocampal volumetry of six hippocampal subfields (see Figure 2 and Table S4). A three-way 2 (group: hippocampal amnesia, control) $\times$ 2 (side: left, right) $\times$ 6 (subfield: dentate gyrus, CA2/3, CA1, subiculum, pre/parasubiculum, uncus) mixed-model ANOVA (with Mauchly's test demonstrating that the assumption of sphericity had been violated for subfield [$\chi^2_{(14)} = 59.583$, $p < 0.001$] and subfield by side [$\chi^2_{(14)} = 78.452$, $p < 0.001$], therefore, degrees of freedom were corrected using Huynh-Feldt estimates $\varepsilon = 0.85$ and 0.64, respectively) demonstrated that there were significant main effects of the group ($F_{(1,34)} = 12.536$, $p = 0.001$), side ($F_{(1,34)} = 13.537$, $p < 0.001$), and subfield ($F_{(4.504,153.152)} = 415.019$, $p < 0.001$). A significant two-way interaction was observed between group and subfield ($F_{(4.504,153.152)} = 4.784$, $p < 0.001$). The three-way interaction was not significant ($F_{(3.679,125.082)} = 0.894$, $p = 0.463$). Planned comparisons demonstrated that this between-group volume loss was isolated to the CA2/3 and CA1 subfields ($F_{(1,34)} = 129.639$, $p < 0.001$, $\eta^2 = 0.792$; and $F_{(1,34)} = 15.330$, $p < 0.001$, $\eta^2 = 0.311$, respectively; Bonferroni-corrected $p = 0.0083$; see Figures 3A and 3B).

At the whole-brain level, there was no significant loss or gain in normalized gray matter volume in the group with hippocampal amnesia relative to controls, based on a voxel-by-voxel contrast of normalized gray matter (two-sample t test, thresholded at $p < 0.05$ family-wise error corrected for multiple comparisons across the whole brain. These results suggest that the memory deficits in the group with hippocampal amnesia were closely linked to specific hippocampal subfield damage, rather than widespread brain pathology.

Subfield pathology is associated with retrograde episodic amnesia

In line with previous findings, neuropsychological assessment in the group with hippocampal amnesia demonstrated focal anterograde visual and verbal memory impairment when compared to the matched control population (see Tables S1 and S2),[31,37,88] alongside specific impairment in the retrieval of internal (episodic) but not external (semantic) memory details.[31,37] An omnibus 2 (group: hippocampal amnesia, control) $\times$ 3 (memory: experimental event memories) $\times$ 2 (memory detail type: internal [episodic], external [semantic]) mixed-model factorial ANOVA was conducted on units of information acquired from the AI for the pre-scanning experimental memories (Mauchly's test confirmed that the assumption of sphericity had not been violated). The results revealed significant main effects of the group ($F_{(1,34)} = 10.983$, $p = 0.002$) and of memory detail type ($F_{(1,34)} = 494.735$, $p < 0.001$) alongside a significant two-way interaction between the group and detail type ($F_{(1,34)} = 10.832$, $p = 0.002$, $\eta^2 = 0.242$), with planned comparisons (alpha criterion corrected for multiple comparisons, $p = 0.025$) revealing a significant loss of internal (episodic) memory detail in the group with hippocampal amnesia compared to the control group ($F_{(1,34)} = 12.055$, $p < 0.001$, $\eta^2 = 0.262$), whereas external (semantic) details were not significantly different ($F_{(1,34)} = 0.001$, $p = 0.973$; see Figures 3C and 3D).

CA2/3 total volume loss predicted episodic amnesia

Next, we found that variability in total CA2/3 but not CA1 volume predicted internal (episodic) detail scores. This was revealed in a stepwise linear regression model with total CA2/3 and CA1 volumes entered as continuous independent variables and internal detail scores as the dependent variable. The model was statistically significant ($F_{(1,34)} = 6.193$, $p = 0.018$). Total CA2/3 volume selectively predicted the amount of internal (episodic) details retrieved ($t = 2.489$, $p = 0.018$, $R^2 = 0.154$, $\beta_1 = 0.393$; see Figure 3E), whereas total CA1 volume was excluded from the model, even when the model was reversed ($t = -0.238$, $p = 0.813$). Mediation analysis using Sobel's test also demonstrated a significant indirect effect of total CA2/3 volume on internal (episodic) detail performance through group membership ($Z = 3.085$; $p = 0.002$; see Tables S1 and S2).

Figure 2. Quantitative 3.0-Tesla (0.5 mm^3 spatial resolution) 3D T2-weighted turbo spin echo images coregistered and averaged with Rician noise estimation and oracle-based discrete cosine transform, were used to conduct whole hippocampal semi-automated volumetry of six hippocampal subfields in the hippocampal amnesia group and in a control group of participants

Denoised sagittal images on the first row illustrate the full longitudinal axis of hippocampi in a (matched) control participant and a participant with amnesia. Each of the white lines (A–E) on the sagittal view of the hippocampus corresponds to six example coronal locations along the anterior-posterior axis. Colored shading on the left-hand side coronal images on rows (A)–(E) under the matched control and participant with amnesia provides examples of the results of applying the hippocampal segmentation protocol in the control and amnesic participant (denoted as '). CA1, cornu ammonis 1; CA2/3, cornu ammonis 2 & 3; DG, dentate gyrus; Pre/para, pre/parasubiculum; SUB, subiculum; and Unc, uncus.

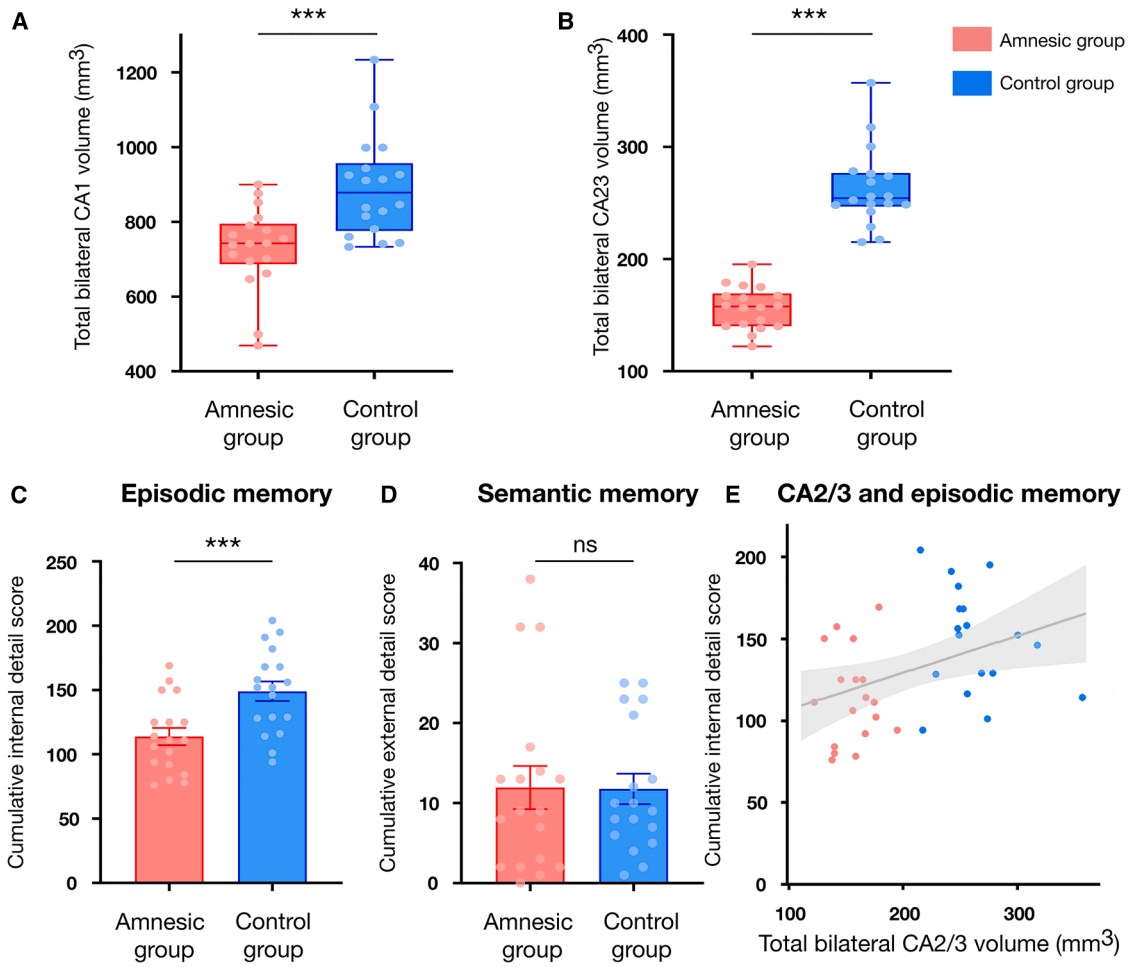

Figure 3. CA2/3 atrophy and impairment of cumulative episodic memory performance in the group with hippocampal amnesia (i.e., single LGI1-LE etiology group)

Hippocampal segmentation was based on 3D T2-weighted turbo spin-echo images, coregistered and averaged with Rician noise estimation and oracle-based discrete cosine transform. Results from hippocampal subfield segmentation in the group with hippocampal amnesia ($n = 18$) relative to the control group. Results from the analyses of hippocampal segmentation are plotted in A and B. (A) Total CA1 and (B) total CA2/3 volumes box-and-whiskers plots in both groups (representing the maximum and minimum values, with the horizontal line denoting the group mean). An omnibus ANOVA revealed a significant (alpha criterion Bonferroni-corrected $p = 0.0083$) reduction in-total CA1 (mean reduction = 18.13%; $F_{(1,34)} = 15.330$, $p < 0.001$, $\eta^2 = 0.311$) and CA2/3 (mean reduction = 40.53%; $F_{(1,34)} = 129.639$, $p < 0.001$, $\eta^2 = 0.792$) volumes in the group with hippocampal amnesia compared to the control group. Results from the analyses of the data obtained from the autobiographical interview (AI) procedure are plotted in (C) and (D). Cumulative (summed across the three experimental memories) episodic memory performance describing both (C) internal (episodic) and (D) external (semantic) details is plotted as a function of group. The group with hippocampal amnesia exhibited a significant deficit in remembering internal (episodic) details relative to controls ($F_{(1,34)} = 12.055$, $p < 0.001$, $\eta^2 = 0.262$), whereas remembering external (semantic) details from the same episodic memories was comparable between the hippocampal amnesia and control groups ($F_{(1,34)} = 0.001$, $p = 0.973$). Error bars represent the standard error of the mean. (E) The scatterplot (with the best-fitting linear regression line) shows that total CA2/3 volume (independent variable) significantly predicts the total number of internal (episodic) details retrieved (dependent variable) across the three experimental memories ($F_{(1,34)} = 6.193$, $p = 0.018$; $t = 2.489$, $p = 0.018$, $R^2 = 0.154$, $\beta_1 = 0.393$). Total CA1 volume was not associated with this relationship ($t = -0.238$, $p = 0.813$). These results also replicate our previous findings in a new cohort of individuals with amnesia. Each dot represents a single data point, with red corresponding to a value for a participant in the group with hippocampal amnesia and blue corresponding to a value for a participant in the control group. *** denotes $p < 0.001$. ns, not significant.

Hippocampal subfield damage selectively disrupts neural responses in the AMN

During the fMRI study, no between-group differences were observed for the intra-scan ratings (see Data S3 and S4), but the post-scan debrief test (see STAR Methods) replicated the pre-scanning behavioral results (see Data S3 and S4). A semantic textual similarity analysis revealed that there was no between-group difference in the cosine similarity of the semantic content for the pre- and post-scanning AMs. This suggests comparable stability in memory content across the two testing sessions in both groups (see supplemental information).

The fMRI data were first analyzed using RDM analysis to test two hypothesized models of neural activity patterns during memory retrieval: (1) a model reflecting similarity across all episodic

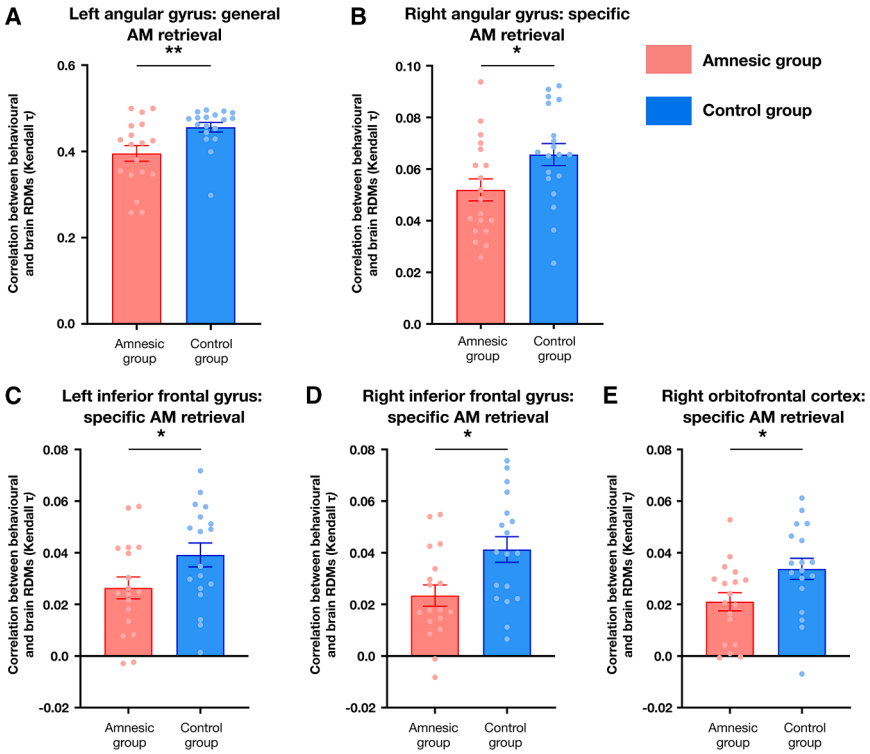

Figure 4. Hippocampal subfield damage selectively impaired the autobiographical memory network

RDMs were used to conduct two model fit analyses: (1) a model reflecting general episodic memory retrieval, independently of the specific episodic memory being remembered; and (2) a model focused on the retrieval of specific episodic memories (see Figures 1D and 1E). As detailed in Data S6, hippocampal subfield pathology did not prevent significant model fits for both hypotheses matrices across the majority of tested cortical regions. Group differences were found; however, in (A), the left angular gyrus for the model specifying representational content during general episodic memory retrieval (group with hippocampal amnesia mean Kendall τ: 0.395 ± 0.078, control group mean Kendall τ: 0.456 ± 0.47; $t_{(34)}$ = 2.830; p = 0.008, Cohen's d = 0.943); and in (B) the right angular cortex (group with hippocampal amnesia mean Kendall τ: 0.0519 ± 0.0045; control group mean Kendall τ: 0.0656 ± 0.0045; $t_{(34)}$ = 2.141; p = 0.040, Cohen's d = 0.714), (C) left inferior frontal gyrus (group with hippocampal amnesia mean Kendall τ: 0.0364 ± 0.0046; control group mean Kendall τ: 0.0391 ± 0.0046; $t_{(34)}$ = 2.038; p = 0.049, Cohen's d = 0.679), (D) right inferior frontal gyrus (group with hippocampal amnesia mean Kendall τ: 0.0233 ± 0.0041; control group mean Kendall τ: 0.0412 ± 0.0049; $t_{(34)}$ = 2.778; p = 0.009, Cohen's d = 0.926), and (E) right orbitofrontal cortex (group with hippocampal amnesia mean Kendall τ: 0.00210 ± 0.0035; control group mean Kendall τ: 0.0337 ± 0.0041; $t_{(34)}$ = 2.357; p = 0.024, Cohen's d = 0.786) for the hypothesis model for specific episodic memories. Error bars correspond to the standard error of the mean (n = 18). * denotes $p < 0.05$; ** denotes $p < 0.01$.

memory retrieval trials, independently of the specific episodic memory being remembered; and (2) a model reflecting similarity across retrieval trials of the same specific episodic memory and dissimilarity between retrieval trials of different memories (see Figures 1D and 1E).

For the first model (general AM retrieval; Figure 4A), significant model fit was observed throughout the AMN in both groups (see Data S6), except for a significant between-group difference in the left angular cortex (group with hippocampal amnesia mean Kendall τ: 0.395 ± 0.078, control group mean Kendall τ: 0.456 ± 0.47; $t_{(34)}$ = 2.830; p = 0.008, Cohen's d = 0.943).

For the second model (mnemonic discriminability; Figures 4B–4E), significant model fit was observed throughout the AMN network in both groups (see Data S6), except for significant between-group differences in the right angular gyrus (rANG; group with hippocampal amnesia mean Kendall τ: 0.0519 ± 0.0045; control group mean Kendall τ: 0.0656 ± 0.0045; $t_{(34)}$ = 2.141; p = 0.040, Cohen's d = 0.714), left inferior frontal gyrus (lIFG; group with hippocampal amnesia mean Kendall τ: 0.0364 ± 0.0046; control group mean Kendall τ: 0.0391 ± 0.0046; $t_{(34)}$ = 2.038; p = 0.049, Cohen's d = 0.679), right inferior frontal gyrus (rIFG; group with hippocampal amnesia mean Kendall τ: 0.0233 ± 0.0041; control group mean Kendall τ: 0.0412 ± 0.0049; $t_{(34)}$ = 2.778; p = 0.009, Cohen's d = 0.926), and the right orbitofrontal cortex (rOFC; group with hippocampal amnesia mean Kendall τ: 0.00210 ± 0.0035; control group mean Kendall τ: 0.0337 ± 0.0041; $t_{(34)}$ = 2.357; p = 0.024, Cohen's d = 0.786). Adjusting for multiple comparisons with Bonferroni correction, the robust effects in the rANG (p = 0.008) and rIFG (p = 0.009) survive correction, whereas effects in the rANG, lIFG, and rOFC fall below the threshold and should thus be considered exploratory pending independent replication.

The fMRI data were also assessed for between-group differences in the mnemonic representational stability of the specific memories, calculated using first-level Fisher-transformed Pearson dissimilarity scores (as a proxy of mnemonic representational stability; Figure 5). An omnibus 2 (group: group with hippocampal amnesia, controls) × 3 (memory: three experimental episodic memories) ANOVA was conducted. Mauchly's test demonstrated that the assumption of sphericity had not been violated. There were significant main effects of the group for the rANG (group with hippocampal amnesia mean: 0.76 ± 0.03; control group mean: 0.68 ± 0.02; $F_{(1,34)}$ = 6.156, p = 0.018, η^2 = 0.153), the rIFG (group with hippocampal amnesia mean: 0.88 ± 0.02; control group mean: 0.81 ± 0.02; $F_{(1,34)}$ = 9.129, p = 0.005, η^2 = 0.213), and the rOFC (group with hippocampal amnesia mean: 0.89 ± 0.02; control group mean: 0.83 ± 0.02; $F_{(1,34)}$ = 6.969, p = 0.012, η^2 = 0.170).

Importantly, no main effect of memory (rANG: $F_{(2,68)}$ = 1.257, p = 0.291, η^2 = 0.036; rIFG: $F_{(2,68)}$ = 0.889, p = 0.416, η^2 = 0.025; and rOFC: $F_{(2,68)}$ = 2.411, p = 0.097, η^2 = 0.066) nor significant group by memory interactions (rANG: $F_{(2,68)}$ = 1.720, p = 0.187, η^2 = 0.048; rIFG: $F_{(2,68)}$ = 0.562, p = 0.573, η^2 = 0.016; and rOFC: $F_{(2,68)}$ = 1.141, p = 0.326, η^2 = 0.032) were observed.

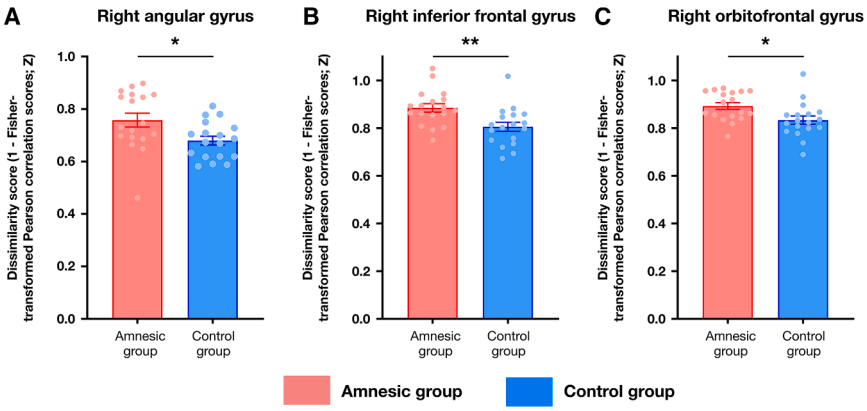

Figure 5. Hippocampal subfield damage was associated with decreased mnemonic stability for specific episodic memories

To investigate these between-group level differences in specific memory representation further, we tested for between-group differences in the Fisher-transformed Pearson correlation scores (as a measure of mnemonic representational stability; lower dissimilarity scores indicate greater voxel population stability for each retrieval trial) corresponding to specific memories from the first-level analysis of the RDMs. This demonstrated that there was a significant main effect of group ($n = 18$; but no main effect of memory or an interaction between the group and memory) in these Fisher-transformed Pearson correlation scores for the (A) right angular gyrus (group with hippocampal amnesia mean: 0.76 ± 0.03; control group mean: 0.68 ± 0.02; $F_{(1,34)} = 6.156$, $p = 0.018$, $\eta^2 = 0.153$); (B) right inferior frontal gyrus (group with hippocampal amnesia mean: 0.88 ± 0.02; control group mean: 0.81 ± 0.02; $F_{(1,34)} = 9.129$, $p = 0.005$, $\eta^2 = 0.213$); and (C) right orbitofrontal gyrus (group with hippocampal amnesia mean: 0.89 ± 0.02; control group mean: 0.83 ± 0.02; $F_{(1,34)} = 6.969$, $p = 0.012$, $\eta^2 = 0.170$). No main effect of memory was seen for the left inferior frontal gyrus (group with hippocampal amnesia mean: 0.87 ± 0.02; control group mean: 0.83 ± 0.02; $F_{(1,34)} = 2.753$, $p = 0.106$, $\eta^2 = 0.075$). * denotes $p < 0.05$; ** denotes $p < 0.01$.

For the lIFG, the ANOVA revealed no significant main effects of the group (group with hippocampal amnesia mean: 0.87 ± 0.02; control group mean: 0.83 ± 0.02; $F_{(1,34)} = 2.753$, $p = 0.106$, $\eta^2 = 0.075$) and memory ($F_{(2,68)} = 0.056$, $p = 0.945$, $\eta^2 = 0.002$), and the group by memory interaction was also non-significant ($F_{(2,68)} = 0.18$, $p = 0.982$, $\eta^2 = 0.001$).

CA2/3 but not CA1 volume predicted the representational stability of episodic memories

Next, we sought to investigate whether there was a causal link between the variability in total CA2/3 and/or total CA1 volumes and the two hypothesis model fits (as measured by Kendall τ for general and specific episodic memory retrieval), as well as the stability in the mnemonic representational similarity across trials (in this case, the averaged Fisher-transformed Pearson dissimilarity scores arising from the first-level analysis). Stepwise regressions were undertaken with total CA2/3 and total CA1 volumes as the independent variables and Kendall τ and averaged Fisher-transformed Pearson correlation values as the dependent variables. Mediation analyses were performed for all regressions using Sobel's test, demonstrating a significant indirect effect of the independent variables on the dependent variable through group membership (see Data S7).

For general episodic memory retrieval, a significant model was identified through stepwise regression ($F_{(1,34)} = 6.452$), where total CA2/3 volume emerged as a selective predictor of episodic memory retrieval model fit in the lANG ($t = 2.540$, $p = 0.016$, $R^2 = 0.159$, $\beta_1 = 0.399$; Figure 7A). Total CA1 volume was excluded from this model even when the order of entry was reversed.

For specific memory retrieval, significant models (Figures 6B–6D) were found for the rANG ($F_{(1,34)} = 5.076$, $p = 0.031$), rIFG ($F_{(1,34)} = 8.605$, $p = 0.006$), and rOFC ($F_{(1,34)} = 6.354$, $p = 0.017$). Crucially, total CA2/3 volume selectively predicted the hypothesis model fit (rANG: $t = 2.253$, $p = 0.031$, $R^2 = 0.130$, $\beta_1 = 0.360$; rIFG: $t = 2.930$, $p = 0.006$, $R^2 = 0.202$, $\beta_1 = -0.449$; and rOFC: $t = 2.521$, $p = 0.017$, $R^2 = 0.157$, $\beta_1 = 0.397$). In all cases, total CA1 volume was excluded from the model, even when the order of entry into the model was reversed (rANG: $t = 0.671$, $p = 0.418$; rIFG: $t = -0.606$, $p = 0.549$; and rOFC: $t = -0.403$, $p = 0.689$). A non-significant stepwise regression model was found for lIFG ($F_{(2,35)} = 2.596$, $p = 0.090$).

When considering the representational stability (where lower dissimilarity scores signify greater trial-by-trial similarity in the neuronal populations supporting those memories, Figures 7A–7C), significant models were found in all three regions (rANG: $F_{(1,34)} = 6.076$, $p = 0.019$; rIFG: $F_{(1,34)} = 10.877$, $p = 0.002$; and, rOFC: $F_{(1,34)} = 6.354$, $p = 0.017$). Notably, the variability in CA2/3 volume predicted the representational stability in all three regions (rANG: $t = -2.465$, $p = 0.019$, $R^2 = 0.152$, $\beta_1 = -0.389$; rIFG: $t = -3.298$, $p = 0.002$, $R^2 = 0.242$, $\beta_1 = -0.492$; and rOFC: $t = -3.382$, $p = 0.002$, $R^2 = 0.252$, $\beta_1 = -0.502$). Once again, total CA1 volume was excluded from the model, even when the order of entry was reversed (rANG: $t = 1.193$, $p = 0.241$; rIFG: $t = 1.626$, $p = 0.113$; and rOFC: $t = 0.449$, $p = 0.656$).

Representational stability predicted the remembering of episodic details associated with personal events

Finally, we wanted to test whether there was a causal relationship between the stability of episodic memory representations (using the first-level Pearson correlation dissimilarity scores) and internal (episodic) memory performance for the experimental memories. The results revealed that the stability of episodic memory representations selectively predicted internal (episodic) memory score in performance in the rIFG ($t = 2.230$, $p = 0.032$, $R^2 = 0.128$, $\beta_1 = 0.357$) and rOFC ($t = -2.189$, $p = 0.036$, $R^2 = 0.124$, $\beta_1 = -0.352$), but not rANG ($t = -1.452$, $p = 0.156$, $R^2 = 0.058$, $\beta_1 = -0.242$; see Figures 7D–7F).

Summary

The results supported and elaborated our *a priori* hypotheses for the fMRI study. The group with hippocampal amnesia showed significantly reduced mnemonic distinctiveness in the rIFG and rOFC, consistent with our prediction of decreased dissimilarity

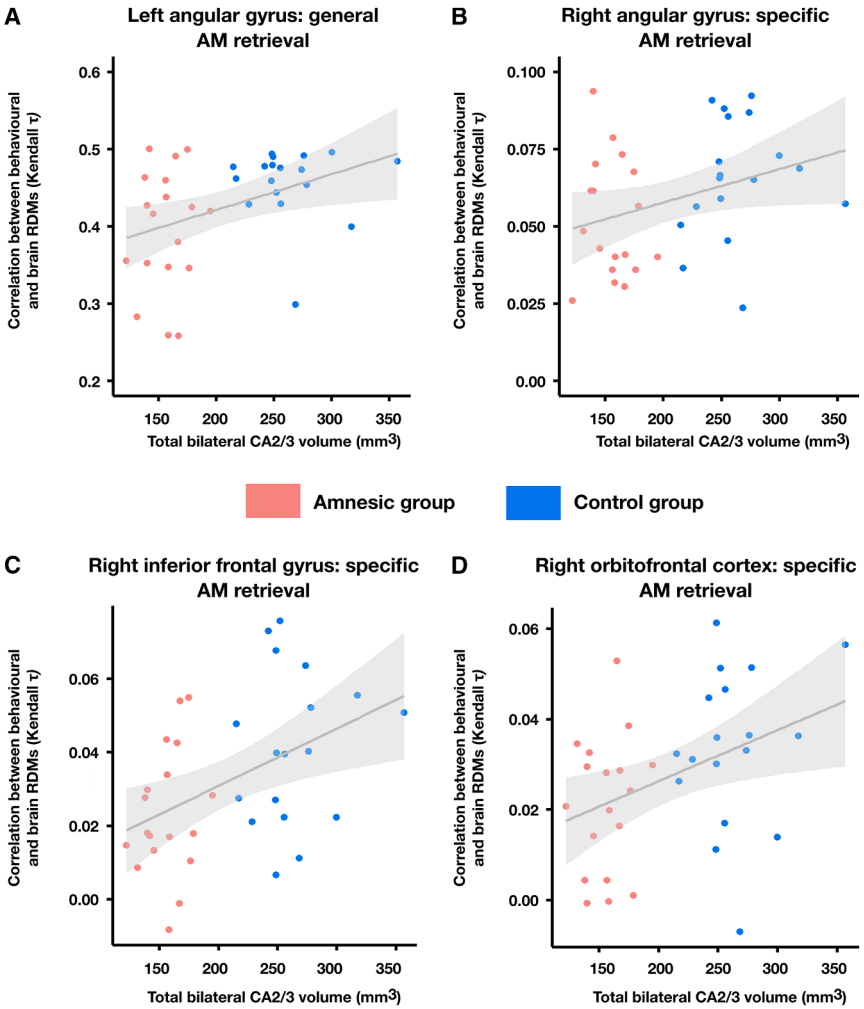

Figure 6. CA2/3 volume predicted RDM model fits across both groups

On the basis of the causal link between the CA2/3 volume and cumulative episodic memory performance, we sought to investigate whether there was also a causal link between the variability in total CA2/3 and/or total CA1 volumes and the two-hypothesis model fits (as measured by Kendall τ; total population n = 36). Stepwise regressions were undertaken with total CA2/3 and total CA1 volumes as the independent variables and Kendall τ correlation values as the dependent variables. (A) For the hypothesis matrix specifying general episodic memory retrieval in the left angular gyrus, a significant model was identified through stepwise regression ($F_{(1,34)} = 6.452$), where total CA2/3 volume emerged as a selective predictor of episodic memory recall ($t = 2.540$, $p = 0.016$, $R^2 = 0.159$, $\beta_1 = 0.399$). Total CA1 volume was excluded from this model, even when the order of entry was reversed ($t = 0.078$, $p = 0.938$). When considering the hypothesis matrix specifying individual memories, significant models were found for the (B) right angular gyrus ($F_{(1,34)} = 5.076$, $p = 0.031$); (C) right inferior frontal gyrus ($F_{(1,34)} = 8.605$, $p = 0.006$); and (D) right orbitofrontal cortex ($F_{(1,34)} = 6.354$, $p = 0.017$). All of these models were then associated with the total CA2/3 volume selectively predicting the hypothesis model fit (rANG: $t = 2.253$, $p = 0.031$, $R^2 = 0.130$, $\beta_1 = 0.360$; rIFG: $t = 2.930$, $p = 0.006$, $R^2 = 0.202$, $\beta_1 = -0.449$; and rOFC: $t = 2.521$, $p = 0.017$, $R^2 = 0.157$, $\beta_1 = 0.397$). In all cases, total CA1 volume was excluded from the model, even when the order of entry into the model was reversed (rANG: $t = 0.671$, $p = 0.418$; rIFG: $t = -0.606$, $p = 0.549$; and rOFC: $t = -0.403$, $p = 0.689$). Graphs show scatterplots (with best-fitting linear regression line) illustrating the relationship between the magnitude of total CA2/3 volume as an independent variable, selectively predicting the model fit scores (total population, n = 36).

between neural representations of distinct episodic memories in hippocampally connected AMN regions. In line with our second hypothesis, greater trial-by-trial stability in the rIFG and rOFC, but not the rANG, predicted higher internal (episodic) detail, supporting the link between stable, differentiated neural patterns and richly detailed recollection. Consistent with our third hypothesis, total CA2/3 volume predicted both general episodic retrieval in the lANG and the retrieval and stability of specific episodic memories in the rANG, rIFG, and rOFC. These findings also support our fourth hypothesis, indicating that reduced CA2/3 volume was associated with both less differentiated neural representations and impaired stability in the trial-by-trial voxel populations that support episodic memory retrieval.

DISCUSSION

A large-scale hippocampal-neocortical network supports episodic memory for autobiographical events and experiences.[3,31,89–93] It is yet unknown how human hippocampal damage affects the representational content in the nodes within this hippocampal-neocortical network. To address this question, we investigated the effects of human hippocampal damage on the representational content of pre-morbid, recently acquired autobiographical memories during retrieval. Results from structural brain neuroimaging and cognitive phenotyping using the AI demonstrated that the hippocampal damage was bilateral, focal, and associated with reduced retrieval of episodic detail. Moreover, variability in total CA2/3 volume predicted the amount of remembered episodic detail. These results replicate previous findings in an entirely new cohort of individuals with amnesia.[31,37] In addition, we found that focal hippocampal pathology was associated with a mild impairment on standardized assessments of anterograde memory, while the group differences in behavior reflected specific memory deficits rather than generalized cognitive dysfunction.[31,37]

Results from fMRI RDM-based analyses revealed that, in line with our first and second hypotheses, hippocampal damage was associated with between-group differences in brain-derived RDM model fit scores, revealing reduced mnemonic dissimilarity (or distinctiveness) in the group with hippocampal amnesia

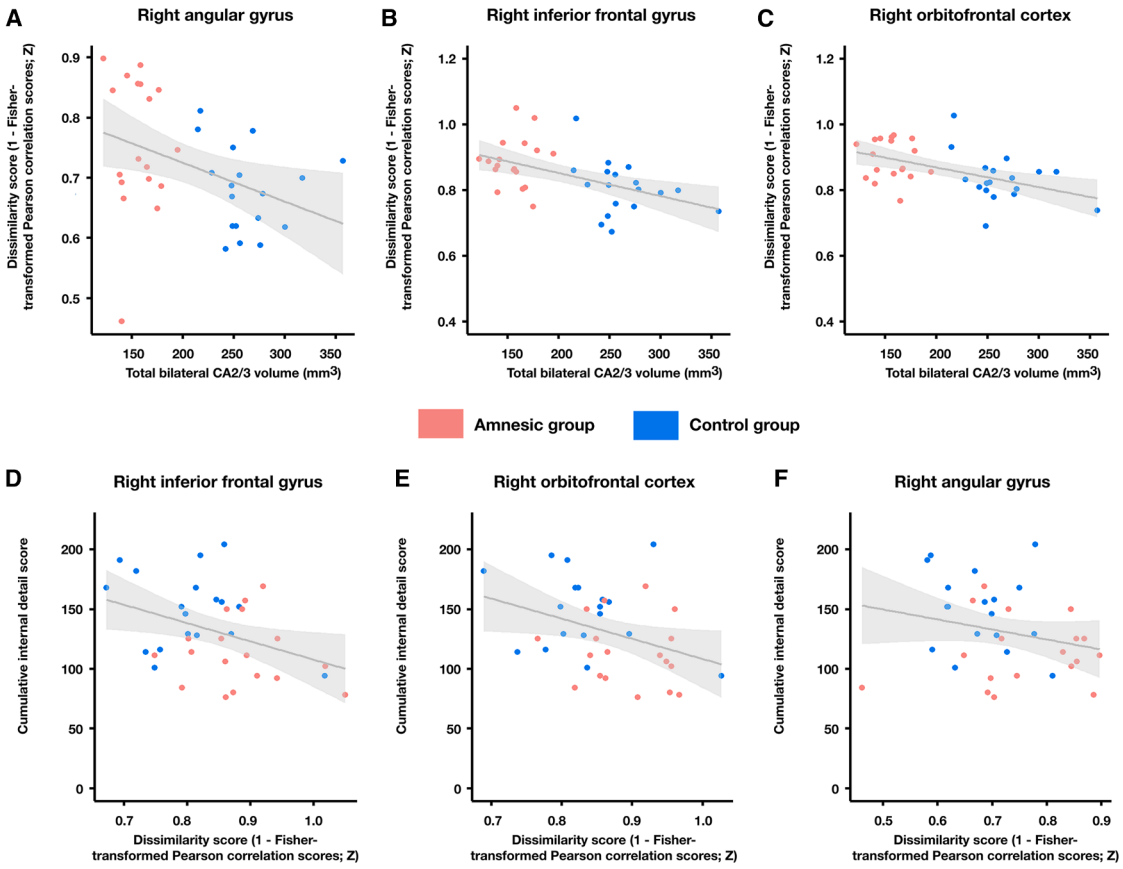

Figure 7. CA2/3 volume predicted episodic memory representational stability, and representational stability predicted the episodic details associated with personal events

When considering the relationship between the total CA2/3 volumes and the averaged dissimilarity scores (where lower scores signify lower trial-by-trial dissimilarity in the voxel populations supporting those memories; calculated by 1: Fisher-transformed Pearson correlation scores), significant models were once again discovered in all three regions: (A) right angular gyrus ($F_{(1,34)} = 6.076$, $p = 0.019$); (B) right inferior frontal gyrus ($F_{(1,34)} = 10.877$, $p = 0.002$); and (C) right orbitofrontal cortex ($F_{(1,34)} = 6.354$, $p = 0.017$). The variability in CA2/3 volume also predicted the averaged Fisher-transformed Pearson scores in all three regions (rANG: $t = -2.465$, $p = 0.019$, $R^2 = 0.152$, $\beta_1 = -0.389$; rIFG: $t = -3.298$, $p = 0.002$, $R^2 = 0.242$, $\beta_1 = -0.492$; and rOFC: $t = -3.382$, $p = 0.002$, $R^2 = 0.252$, $\beta_1 = -0.502$). Once again, total CA1 volume was excluded from the model even when the order of entry was reversed (rANG: $t = 1.193$, $p = 0.241$; rIFG: $t = 1.626$, $p = 0.113$; and rOFC: $t = 0.449$, $p = 0.656$). Graphs show scatterplots (with best-fitting linear regression line) illustrating the relationship between the magnitude of total CA2/3 volume as an independent variable, selectively predicting the averaged Fisher-transformed Pearson scores for the three experimental memories. Averaged mnemonic representational dissimilarity scores across recall trials were used as the independent variable in a linear regression with cumulative internal (episodic) detail score as the dependent variable. We found that the similarity of episodic memory representations selectively predicted internal (episodic) memory score in the (D) rIFG ($t = 2.230$, $p = 0.032$, $R^2 = 0.128$, $\beta_1 = 0.357$) and (E) rOFC ($t = -2.189$, $p = 0.036$, $R^2 = 0.124$, $\beta_1 = -0.352$), but not (F) rANG ($t = -1.452$, $p = 0.156$, $R^2 = 0.058$, $\beta_1 = -0.242$). Graphs show scatterplots (with best-fitting linear regression line) illustrating the relationship between the magnitude of the dissimilarity scores for the three episodic memories (per participant) as the independent variable, selectively predicting the cumulative internal (episodic) scores for the three experimental memories (total population $n = 36$).

across a limited number of cortical regions within the AMN. Specifically, between-group differences in the representation of the episodic memory retrieval state (versus the baseline counting state) were limited to the lANG, whereas differences in the representation of specific episodic memories were found in the rANG, rOFC, lIFG, and rIFG. This circumscribed effect is notable, given that the hippocampus is an important hub region,[79–82] and suggests that hippocampal damage can have a limited, rather than widespread, impact on memory representations in the cortical regions. These more limited effects on the cortical network nodes align with previous graph theoretical analyses of multiple resting-state networks, which showed that the disruptive effects of focal CA3 damage led to limited effects on network topology.[31] Importantly, hippocampal subfield volume predicted the magnitude of dissimilarity between specific episodic memories, with the variability in the model fit across all regions specifically predicted only by total CA2/3 volumes. Hence, we show that CA2/3 not only has a critical role in supporting the retrieval of episodic memories but also in supporting the maximal dissimilarity in the neocortical neural representation of competing memories.

Having discovered the impact of hippocampal damage on the representation of dissimilar episodic memories, we tested our third hypothesis by examining the effects of hippocampal

pathology on the stability of specific mnemonic representation and[70] found that, compared with the control group, the group with hippocampal amnesia had increased trial-by-trial dissimilarity in the voxel patterns within the rANG, rOFC, and rIFG; in addition, the variability in these values was predicted by total CA2/3 volume. Crucially, we discovered that lower trial-by-trial dissimilarity in the rOFC and rIFG was predictive of the retrieval of greater episodic memory detail. In support of our fourth hypothesis, reduced CA2/3 volumes were not only associated with less differentiated neural representations of specific episodic memories but also with an impairment in the stability of the trial-by-trial voxel populations that supported those episodic memories.

Both distinctiveness and stability are crucial for memory performance, and have been described as separate properties of neural representations.[70] These effects align with the dual role of CA3 in supporting computations that make overlapping experiences more distinct (pattern separation)[78] and those that code relationships across items to increase overlap (pattern completion).[38,83,90,94–97] In healthy adults, CA3 volume has been previously found to scale linearly with the degree of differentiation between neuronal voxel populations within the hippocampus for specific episodic memories, which contributes to efficient pattern separation.[64] Reduced CA2/3 volumes might therefore be associated with less efficient pattern separation,[77] leading to reduced dissimilarity between competing episodic memories within the hippocampus, whereas voxel population instability could indicate compromised pattern completion. It is conceivable that decreased mnemonic overlap within CA3 is associated with increased mnemonic competition within the neocortex, potentially leading to reduced episodic memory re-experiencing.[64] Here, we demonstrated that the stability of those neocortical voxel ensembles was linked with CA2/3 volume loss, and this instability was indirectly associated with the retrieval of less re-experiential and detailed episodic memories. CA2/3 pathology may, therefore, disrupt the balance between pattern separation and completion computations, which underlie successful episodic memory retrieval. Furthermore, the dentate gyrus did not exhibit significant volume loss in the group with hippocampal amnesia, which raises the possibility that it continued to support pattern separation during the retrieval of specific autobiographical memories (an essential computational operation underlying mnemonic distinctiveness), although its contribution may nevertheless be altered by CA2/3 and CA1 pathology.

Next, we consider in greater detail how reduced dissimilarity in the affected nodes of the AMN (lANG, rANG, lIFG, rIFG, and rOFC) is likely to be translated into impaired episodic memory. In the ANG, we found that lANG was implicated in the state of episodic memory retrieval, whereas the rANG was implicated in the representation of specific episodic memories. The ANG maintains extensive connections with multiple neocortical regions and plays a crucial role in memory tasks that require detailed recollection or complex integration of information across sensory modalities.[5,98–102] Emerging evidence suggests distinct functional roles for the left and right hemispheric components. The lANG is functionally connected with the dorsomedial PFC subsystem[103] of the default mode network (DN),[104] a subsystem that has been implicated in subjective elements of confident recollection rather than the retrieval of the objective context.[103,105] The lANG may, in alignment with our RDM-based results reported here, support the generalized and subjective aspects of recollective confidence and re-experiential richness,[106] rather than the objective recollection of details forming that specific event.[103,107] In contrast, the rANG appears to have greater functional connectivity with components of the MTL subsystem of the DN during episodic memory retrieval.[105] The MTL subsystem is implicated in the retrieval of source memories[105] and the retrieval of specific temporal order,[108] with the rANG having a specific role in supporting the objective retrieval of specific episodic memory details.[103] Our results would seem to corroborate a putative role of the rANG in representing specific episodic mnemonic details, given that hippocampal damage in the group with hippocampal amnesia was associated with a diminished ability to represent distinct episodic memories. Hence, it would appear that diminished mnemonic distinctiveness impaired both the subjective experience of episodic memories supported by the lANG and the remembering of specific episodic details mediated by the rANG. Studying specific subdivisions within the ANG may reveal new insights into the mechanisms behind episodic memory impairments.

Hippocampal pathology also impaired specific mnemonic representation in the lIFG, rIFG, and rOFC. These findings align with previous studies that have shown that IFG is crucial for episodic memory,[109–113] and has also been implicated in other cognitive control processes, including task monitoring,[114] cognitive control,[115–117] representing imagined stimuli,[116,118,119] suppressing irrelevant memories,[120] and sensitivity to cue specification.[121] The rOFC was also implicated in the representation of specific episodic memories, which is in line with previous studies of episodic learning[122–125] and retrieval,[126] where univariate BOLD signal increase within the OFC has been linked to subsequent memory performance.[122] The hippocampus and OFC interact closely during episodic memory tasks, with the hippocampus providing crucial contextual information to the OFC to facilitate the integration of episodic details within broader cognitive frameworks.[127,128] Therefore, hippocampal damage may disrupt the integration of context-specific memory representations to the OFC,[129] thereby impeding the formation of a coherent cognitive representation of the memory.[129–131] Support for this contention comes from OFC lesion studies that have revealed difficulty in distinguishing between relevant and irrelevant memory traces, alongside content misattribution.[125,132–134] The OFC appears to be recruited after other components of the AMN, which suggests that it exerts important evaluative and integrative functions central to memory-based decision-making processes,[126] thereby functioning to mediate between specific memories.[135] In summary, reduced episodic mnemonic discrimination within IFG and OFC was associated with less fine-grained episodic detail, perhaps due to the inability to represent distinct and/or stable memories that are required for supporting these later-stage monitoring or evaluative processes.

More broadly, the ANG, OFC, and IFG form part of the frontoparietal control network (FPCN),[104,136,137] which contributes to executive control and guiding goal-based actions.[138] The FPCN is closely connected with the DN and the dorsal attention network (DAN).[139] The FPCN can be fractionated into two

distinct subsystems using resting state-fMRI: (1) FPCN subsystem A ($FPCN_A$; comprised in part by the OFC and ANG), which is closely associated with the DN; and (2) FPCN subsystem B ($FPCN_B$; comprised, in part, by the IFG), which is closely associated with the DAN. Functionally, the $FPCN_A$ regions are associated with tasks requiring introspective attention away from perceptual input[140,141] and episodic memory.[142–144] Given that the DN facilitates the integration of conceptual-associative knowledge into current thought and perception,[145–147] hippocampal damage could potentially destabilize the representation of internally generated mnemonic re-experiencing. $FPCN_B$ regions appear closely related to cognitive control by supporting the encoding of task-relevant information, including task rules and their relationship to expected reward outcomes[136,148–151] as well as through top-down modulation of the DAN.[152,153] Hippocampal damage may impair the ability of the $FPCN_B$ to utilize distinct and/or stable mnemonic information in order to maintain the top-down attention on specific episodic memory retrieval.

Importantly, our data show that hippocampal damage did not eliminate specific mnemonic representations across other nodes within the AMN (as detailed in the Data S6). This is not unexpected, especially given that selective hippocampal damage impairs certain aspects of memory retrieval, yet it does not prevent remembering all details related to specific episodic memories.[22,23,25–28,30,31,37,78,154] We interpret these data as showing that hippocampal subfield damage leads to degraded rather than entirely non-discriminable autobiographical memory representations. Non-discriminable representations could suggest a complete functional disconnection between the hippocampus and the cortex, whereas degraded but above-chance representations can indicate that hippocampal-cortical circuits maintain some integrity despite subfield damage, with reduced fidelity rather than complete loss.[90,155] These findings align with other studies that show preserved but degraded neural representations in amnesia. For example, patients with developmental amnesia show above-chance but reduced neural pattern similarity during scene processing,[156] and MTL damage is associated with the retention of some categorical information in visual cortex despite impaired episodic memory.[157] This pattern suggests that partial hippocampal damage typically produces graded rather than all-or-none representational impairments.

The lack of group differences in AM distinctiveness and stability within the ventromedial prefrontal cortex (vmPFC) is also particularly notable. The vmPFC is involved in self-referential and schema-based processing,[145,158–162] particularly for memories of personal significance,[163] and guides strategic search processes for specific autobiographical memories.[164–167] Recent electrophysiological studies, including magnetoencephalography (MEG) and intracranial recordings,[126,168] demonstrate that activity in the vmPFC precedes the hippocampus and other network hubs during autobiographical memory retrieval. Our findings are consistent with this early-stage, orchestrating role for the vmPFC, and suggest that hippocampal subfield pathology does not disrupt the integrity of vmPFC-mediated representations. This supports the view that the vmPFC can initiate and maintain schematic or self-referential aspects of memory retrieval even in the presence of hippocampal dysfunction, which aligns with the hierarchical and interactive models of autobiographical memory retrieval.[165,169]

Some representational accounts posit that the hippocampus is required for episodic retrieval where the memory has spatial detail and context-specific content.[3,5,40,41,170] Accordingly, hippocampal damage could render episodic memories "gist-like" in nature, yet these memories still persist as discrete events.[3,5,40,41,170] Given that the retrieval of richly re-experiential memories requires coordination of multiple cortical regions,[3,89–93] the retrieval of the gist or context of a memory could be hippocampal-independent.[3,5,40,41,170] Under such an account, the hippocampus is critical for integrating sensory, perceptual, and conceptual information into a cohesive experience.[1–5] Incorporating this account into what is known about CA3-mediated computations may explain our findings in terms of residual functionality. Specifically, the hippocampal pathology may prevent the representation of distinct and/or stable memories, resulting in the observed episodic impairments, but still permits some degree of mnemonic discriminability to support memory retrieval. This interpretation aligns with the idea that hippocampal damage can affect the richness and detail of memories rather than completely abolishing episodic remembering, and it provides a potential mechanism for the observed preservation of gist-like memory retrieval in the context of hippocampal pathology.

An alternative interpretation of our findings invokes mnemonic interference as a key mechanism underlying the emergence of autobiographical amnesia. According to the classical hypothesis of mnemonic interference, amnesia results from heightened vulnerability to competing memory traces, particularly during contextual discrimination.[171,172] Our evidence of reduced representational stability and distinctiveness in cortical regions can be interpreted as a neural signature of this increased susceptibility to interference. Hippocampal subfield damage may render memories more susceptible to mutual interference during cortical representation. This extends beyond item-specific interference to reflect fundamental disruption of memory consolidation processes, consistent with evidence that amnesia involves heightened susceptibility to non-specific retroactive interference, where any post-learning activity can disrupt memory formation.[173–175] Future studies should test whether targeted reduction of context-based interference (e.g., through environmental cue optimization) can improve representational distinctiveness and stability in hippocampal pathology.

Our findings also overlap with evidence from established rodent models of hippocampal dysfunction, albeit within CA1. Aged rats exhibit multistable CA1 place fields, whereby place field maps remain accurate and stable within individual recording sessions but frequently undergo complete rearrangements between sessions, leading to deficits in spatial memory performance.[176–179] Human fMRI studies have found analogous findings, with reduced pattern stability in CA1 correlated with impaired spatial discrimination and worse memory performance in older adults.[180] The pattern instability in aging reflects compromised input from upstream hippocampal circuits, particularly the CA3-to-CA1 projections. Thus, in our study, focal damage to CA2/3 likely disrupts these critical upstream computations, impairing pattern separation/completion mechanisms essential for the stabilization of

spatiotemporal event representations in a manner that parallels the multistable cognitive maps observed in aged rodents.[181,182] This dysfunction may bias the hippocampal network toward pattern completion at the expense of pattern separation, potentially having relevance for understanding the reduced distinctiveness and stability of cortical memory representations that we observed in LGI1-LE.

We also replicated previous findings on the anatomical effects of the LGI1-LE etiology, thereby confirming that the damage was limited to bilateral hippocampal regions. A prior study involving eighteen individuals with the same, single etiology reported bilateral focal CA3 volume loss (~28% volume loss compared to controls).[31,37] In the current study, there was an almost 40% reduction in CA2/3 volume compared to the control group. One source of this notional difference is that CA2 and CA3 were not separately delineated due to technical reasons, including the use of lower field-strength MRI (3.0-Tesla vs. 7.0-Tesla) and differences in other acquisition parameters, which led to differences in the biophysical appearance of the hippocampal subfields. Delineation of the hippocampal subfields in the current study was also performed with a semi-automated segmentation pipeline on the 3.0-Tesla dataset, with manual validation versus a protocol limited to manual segmentation on the 7.0-Tesla dataset. Contrary to previous results, the current cohort also demonstrated significant CA1 atrophy. The current data, however, remain comparable with those previous results. The previous non-significant CA1 result was observed in the context of a Holm-Bonferroni corrected alpha-criterion,[31,37] yet the proportion of volume loss in CA1 reported here from 18 individuals with the same presentation and etiology is similar (18% in the current study and 15% previously). CA1 atrophy is not necessarily unexpected, as there is evidence of neuronal loss in both CA3 and CA1 following seizures in homozygous LGI1 knockout mice.[183] Further data will be needed to adjudicate as to whether significant volume loss in CA1 is a feature of LGI1-LE. In line with prior studies, we also found no supra-threshold clusters of gray matter volume loss in the group with hippocampal amnesia compared to the controls. Together, the hippocampal segmentation and whole-brain data align with those reported by other laboratories.[31,37,48,54,55,184]

Notably, the CA1 volume loss was not linked with the behavioral and neural measures. Despite the limited statistical power due to the small range of CA1 volume loss, limiting the effectiveness of linear modeling, we address several non-exclusive factors that can also account for these null effects. First, prior reports have noted that variability in CA2/3 volume is associated with improved episodic (internal) detail performance.[185,186] In contrast, recently acquired AMs (i.e., less than 2 weeks old) have been decoded within CA1, whereas the representation of remote memories (which includes the test memories reported here) was preferentially decoded within the posterior CA3 and DG.[44] Accordingly, the current results could arguably align with the view that CA1 provides less support for remote AMs. Second, the chronic nature of LGI1-LE differs fundamentally from acute CA1 lesions reported in transient global amnesia, where profound autobiographical memory deficits occur immediately following impaired CA1 function.[187] In LGI1-LE, functional reorganization and compensatory mechanisms may develop over time, and enable alternative hippocampal-cortical pathways to maintain memory function despite CA1 damage. Relatedly, the specific pathology in LGI1-LE is known to affect CA2/3 preferentially,[188] with CA1 involvement being less marked, which may further reduce the likelihood of detecting CA1-behavior relationships in this cohort. Indeed, if CA1 volume loss occurs without proportional functional consequences, the structural damage may reflect the downstream effects of CA3 dysfunction rather than primary CA1 pathology. Third, the functional specialization of CA1 may not align with the cognitive demands of the current task. Evidence shows that CA1 is associated with experience integration, temporal context specification, and source memory representation.[189–191] Furthermore, computational models suggest that CA1 performs linear integration of CA3 and entorhinal inputs (unlike the nonlinear attractor dynamics identified with CA3) and is critical for temporal binding and pattern completion when inputs are degraded. The current fMRI task focused on differentiating between specific episodic memories within 15-s time frames. These operations emphasize CA3-supported pattern separation of complete, well-consolidated memories rather than the specialized functions of CA1 in temporal binding, degraded input processing, or source memory integration. This task design may therefore explain the absence of CA1 volume-function relationships. Fourth, preserved CA3 function may compensate for CA1 damage through alternative neural pathways. CA3 neurons have direct subcortical efferents that bypass CA1, and intact CA3 regions can project to ventral CA1 areas via longitudinal connections. Given that our LGI1-LE cohort showed focal CA2/3 damage with relatively preserved DG, compensatory circuits may maintain autobiographical memory function despite CA1 volume loss, masking structure-function relationships that would be evident in more complete hippocampal lesions.

In terms of theoretical significance for accounts of episodic memory, our results accord with recent reconstructive models of hippocampal function,[1–5,41] whereby hippocampal pathology did not prevent the representation of discrete autobiographical events; instead, it impaired the cortical dissimilarity and stability of specific autobiographical memories in only a small subset of AMN nodes. Although we were limited by voxel size in this study, assessing mnemonic dissimilarity within individual hippocampal subfields would be critical for determining whether a failure of pattern separation occurs within CA2/3. Moreover, to ensure hippocampal involvement, we specifically chose to evaluate memories from a recent time point that, according to multiple models of hippocampal function, should still rely on hippocampal processing for retrieval.[4,5,12,41,44,192–194] Accordingly, the current data support theories that place the hippocampus as a central coordinating hub within the AMN, with hippocampal damage altering mnemonic representations in distal cortical regions.[1–5,21] In future work, it will be crucial to establish whether memories arising from more distant time points have the same pattern of decreased mnemonic dissimilarity as these hippocampal-dependent memories.[12]

To conclude, our results have addressed a key question: how does focal hippocampal damage, associated with episodic amnesia, affect the representational content and brain network that underlies autobiographical memories? We found that hippocampal pathology prevented the distinct and stable representation of episodic memories in a sparse number of cortical

components of the AMN, albeit ones with critical functions to episodic memory retrieval. We were able to relate the stability of voxel activity patterns across each memory retrieval trial to the amount of episodic memory details retrieved, thereby providing, for the first time, the first direct neural correlation between focal hippocampal dysfunction, altered mnemonic representational content, and episodic amnesia. Future research should explore the temporal dynamics of cortical representations during memory formation and retrieval to understand better how hippocampal-cortical interactions enable flexible event component reuse. In addition, investigating how different cortico-hippocampal networks represent specific event components during online experience and memory retrieval could enhance our understanding of how the brain scaffolds memory for various high-level event elements.

Limitations of the study

The present study has several limitations. The 3.0-Tesla field strength utilized lacked sufficient spatial resolution to apply RDM analysis to individual hippocampal subfields. Given the unidirectional flow of information through the hippocampal trisynaptic circuit, quantifying the distinctiveness and stability of AM neural representation at the subfield level could reveal where AM misrepresentation occurs within the hippocampus, and, consequently, how specific neurocomputational processes are affected. Enhanced spatial resolution could also identify additional cortical regions where hippocampal damage results in impaired AM representation. Second, we did not assess the distinctiveness and stability of remote AMs (~15–20 years old). Future investigations could examine remote AM representations to determine whether hippocampal damage renders these older memories susceptible to misrepresentation. Finally, the experimental design was not optimized for assessing functional or effective connectivity during AM remembering. Accordingly, future studies could adapt our experimental approach to examine in greater detail how hippocampal damage affects the dynamic connectivity patterns underlying AM retrieval.

RESOURCE AVAILABILITY

Lead contact

Further information and requests for resources should be directed to the lead contact, Thomas D. Miller (t.d.miller@ucl.ac.uk).

Materials availability

This study did not generate new, unique reagents.

Data and code availability

- The data reported in this study are not available for open distribution to comply with restrictions imposed by the local research ethics committee, institutional research governance policies, and UK data protection regulation (GDPR and Data Protection Act 2018). For further details on the restrictions related to data sharing, please contact the lead contact.
- No original code was generated for this study.

ACKNOWLEDGMENTS

This work is dedicated to Prof. Eleanor Maguire, who was involved throughout the experiment, demonstrating her courage and dedication to cognitive neuroscience. Eleanor passed away before manuscript completion. The work reported here represents one of Eleanor's final empirical contributions to the neuroscience of the hippocampus and episodic memory. Eleanor's legacy will be continued by her trainees and collaborators. We would like to thank Prof. Cathy Price for her comments on the manuscript. T.D.M. is supported by the Wellcome Trust (Grant number: 222913/Z/21/Z). A.E.H. is supported by the Medical Research Council (MR/X022013/1 and MR/V007173/1) and the National Institute for Health Research (NIHR) Oxford Health Biomedical Research Centre (BRC).

AUTHOR CONTRIBUTIONS

Conceptualization, methodology, investigation, data curation, formal analysis, validation, funding acquisition, resources, project administration, visualization, and writing – original draft, reviewing and editing, T.D.M.; methodology, software, formal analysis, and writing – reviewing and editing, A.L.H.; methodology, software, and writing – reviewing and editing, Y.I.W.; formal analysis and writing – reviewing and editing, J.H.Z.; resources and writing – reviewing and editing, A.E.H.; resources and writing – reviewing and editing, E.C.; resources and writing – reviewing and editing, T.A.P.; resources and writing – reviewing and editing, M.S.Z.; formal analysis, visualization, writing – original draft, and reviewing and editing, C.R.R.; and conceptualization, methodology, formal analysis, funding acquisition, resources, project administration, and supervision, E.A.M.

DECLARATION OF INTERESTS

The authors declare no competing interests.

STAR★METHODS

Detailed methods are provided in the online version of this paper and include the following:

- KEY RESOURCES TABLE
- EXPERIMENTAL MODEL AND SUBJECT DETAILS
  - Participant details
- METHOD DETAILS
  - Neuropsychological assessment
  - Neuropsychology statistical analyses
  - Autobiographical interview
  - Scoring and reliability
  - Autobiographical interview statistical analysis
  - Stimuli and experimental paradigm
  - Data acquisition
- QUANTIFICATION AND STATISTICAL ANALYSIS
  - Whole-brain voxel-by-voxel morphometry and cortical parcellation
  - Anatomical segmentation of hippocampal subfields
  - Hippocampal subfield segmentation statistical analysis
  - Autobiographical network definition
  - Functional magnetic resonance pre-processing
  - Representational similarity analysis
  - Model matrix comparisons
  - Statistical analyses

SUPPLEMENTAL INFORMATION

Supplemental information can be found online at https://doi.org/10.1016/j.celrep.2025.116527.

Received: March 19, 2025
Revised: August 13, 2025
Accepted: October 18, 2025
Published: November 10, 2025

REFERENCES

1. Nadel, L., and Moscovitch, M. (1997). Memory consolidation, retrograde amnesia and the hippocampal complex. Curr. Opin. Neurobiol. *7*, 217–227. https://doi.org/10.1016/s0959-4388(97)80010-4.
2. Hassabis, D., and Maguire, E.A. (2009). The construction system of the brain. Philos. Trans. R. Soc. Lond. B Biol. Sci. *364*, 1263–1271. https://doi.org/10.1098/rstb.2008.0296.
3. Maguire, E.A., and Mullally, S.L. (2013). The hippocampus: a manifesto for change. J. Exp. Psychol. Gen. *142*, 1180–1189. https://doi.org/10.1037/a0033650.
4. Winocur, G., and Moscovitch, M. (2011). Memory transformation and systems consolidation. J. Int. Neuropsychol. Soc. *17*, 766–780. https://doi.org/10.1017/S1355617711000683.
5. Moscovitch, M., Cabeza, R., Winocur, G., and Nadel, L. (2016). Episodic Memory and Beyond: The Hippocampus and Neocortex in Transformation. Annu. Rev. Psychol. *67*, 105–134. https://doi.org/10.1146/annurev-psych-113011-143733.
6. St Jacques, P.L., Kragel, P.A., and Rubin, D.C. (2011). Dynamic neural networks supporting memory retrieval. Neuroimage *57*, 608–616. https://doi.org/10.1016/j.neuroimage.2011.04.039.
7. McCormick, C., St-Laurent, M., Ty, A., Valiante, T.A., and McAndrews, M.P. (2015). Functional and effective hippocampal-neocortical connectivity during construction and elaboration of autobiographical memory retrieval. Cereb. Cortex *25*, 1297–1305. https://doi.org/10.1093/cercor/bht324.
8. Suddendorf, T., and Corballis, M.C. (2007). The evolution of foresight: What is mental time travel, and is it unique to humans? Behav. Brain Sci. *30*, 299–351, discussion 313-251. https://doi.org/10.1017/S0140525X07001975.
9. Takehara-Nishiuchi, K. (2020). Prefrontal-hippocampal interaction during the encoding of new memories. Brain Neurosci. Adv. *4*, 2398212820925580. https://doi.org/10.1177/2398212820925580.
10. Addis, D.R., Moscovitch, M., Crawley, A.P., and McAndrews, M.P. (2004). Recollective qualities modulate hippocampal activation during autobiographical memory retrieval. Hippocampus *14*, 752–762. https://doi.org/10.1002/hipo.10215.
11. Yazar, Y., Bergström, Z.M., and Simons, J.S. (2017). Reduced multimodal integration of memory features following continuous theta burst stimulation of angular gyrus. Brain Stimul. *10*, 624–629. https://doi.org/10.1016/j.brs.2017.02.011.
12. Bonnici, H.M., and Maguire, E.A. (2018). Two years later - Revisiting autobiographical memory representations in vmPFC and hippocampus. Neuropsychologia *110*, 159–169. https://doi.org/10.1016/j.neuropsychologia.2017.05.014.
13. Bonnici, H.M., Richter, F.R., Yazar, Y., and Simons, J.S. (2016). Multimodal Feature Integration in the Angular Gyrus during Episodic and Semantic Retrieval. J. Neurosci. *36*, 5462–5471. https://doi.org/10.1523/JNEUROSCI.4310-15.2016.
14. Reagh, Z.M., and Ranganath, C. (2023). Flexible reuse of cortico-hippocampal representations during encoding and recall of naturalistic events. Nat. Commun. *14*, 1279. https://doi.org/10.1038/s41467-023-36805-5.
15. Yarkoni, T., Speer, N.K., and Zacks, J.M. (2008). Neural substrates of narrative comprehension and memory. Neuroimage *41*, 1408–1425. https://doi.org/10.1016/j.neuroimage.2008.03.062.
16. Binder, J.R., and Desai, R.H. (2011). The neurobiology of semantic memory. Trends Cogn. Sci. *15*, 527–536. https://doi.org/10.1016/j.tics.2011.10.001.
17. Binder, J.R., Desai, R.H., Graves, W.W., and Conant, L.L. (2009). Where is the semantic system? A critical review and meta-analysis of 120 functional neuroimaging studies. Cereb. Cortex *19*, 2767–2796. https://doi.org/10.1093/cercor/bhp055.
18. Reagh, Z.M., and Ranganath, C. (2018). What does the functional organization of cortico-hippocampal networks tell us about the functional organization of memory? Neurosci. Lett. *680*, 69–76. https://doi.org/10.1016/j.neulet.2018.04.050.
19. Ranganath, C., and Ritchey, M. (2012). Two cortical systems for memory-guided behaviour. Nat. Rev. Neurosci. *13*, 713–726. https://doi.org/10.1038/nrn3338.
20. Zeidman, P., and Maguire, E.A. (2016). Anterior hippocampus: the anatomy of perception, imagination and episodic memory. Nat. Rev. Neurosci. *17*, 173–182. https://doi.org/10.1038/nrn.2015.24.
21. Steinvorth, S., Corkin, S., and Halgren, E. (2006). Ecphory of autobiographical memories: an fMRI study of recent and remote memory retrieval. Neuroimage *30*, 285–298. https://doi.org/10.1016/j.neuroimage.2005.09.025.
22. Bayley, P.J., Hopkins, R.O., and Squire, L.R. (2003). Successful recollection of remote autobiographical memories by amnesic patients with medial temporal lobe lesions. Neuron *38*, 135–144. https://doi.org/10.1016/s0896-6273(03)00156-9.
23. Bayley, P.J., Hopkins, R.O., and Squire, L.R. (2006). The fate of old memories after medial temporal lobe damage. J. Neurosci. *26*, 13311–13317. https://doi.org/10.1523/JNEUROSCI.4262-06.2006.
24. Kirwan, C.B., Bayley, P.J., Galván, V.V., and Squire, L.R. (2008). Detailed recollection of remote autobiographical memory after damage to the medial temporal lobe. Proc. Natl. Acad. Sci. USA *105*, 2676–2680. https://doi.org/10.1073/pnas.0712155105.
25. Noulhiane, M., Piolino, P., Hasboun, D., Clemenceau, S., Baulac, M., and Samson, S. (2007). Autobiographical memory after temporal lobe resection: neuropsychological and MRI volumetric findings. Brain *130*, 3184–3199. https://doi.org/10.1093/brain/awm258.
26. Squire, L.R., van der Horst, A.S., McDuff, S.G.R., Frascino, J.C., Hopkins, R.O., and Mauldin, K.N. (2010). Role of the hippocampus in remembering the past and imagining the future. Proc. Natl. Acad. Sci. USA *107*, 19044–19048. https://doi.org/10.1073/pnas.1014391107.
27. Viskontas, I.V., McAndrews, M.P., and Moscovitch, M. (2000). Remote episodic memory deficits in patients with unilateral temporal lobe epilepsy and excisions. J. Neurosci. *20*, 5853–5857. https://doi.org/10.1523/JNEUROSCI.20-15-05853.2000.
28. Addis, D.R., Moscovitch, M., and McAndrews, M.P. (2007). Consequences of hippocampal damage across the autobiographical memory network in left temporal lobe epilepsy. Brain *130*, 2327–2342. https://doi.org/10.1093/brain/awm166.
29. McCormick, C., Moscovitch, M., Valiante, T.A., Cohn, M., and McAndrews, M.P. (2018). Different neural routes to autobiographical memory recall in healthy people and individuals with left medial temporal lobe epilepsy. Neuropsychologia *110*, 26–36. https://doi.org/10.1016/j.neuropsychologia.2017.08.014.
30. St-Laurent, M., Moscovitch, M., and McAndrews, M.P. (2016). The retrieval of perceptual memory details depends on right hippocampal integrity and activation. Cortex *84*, 15–33. https://doi.org/10.1016/j.cortex.2016.08.010.
31. Miller, T.D., Chong, T.T.J., Aimola Davies, A.M., Johnson, M.R., Irani, S.R., Husain, M., Ng, T.W., Jacob, S., Maddison, P., Kennard, C., et al. (2020). Human hippocampal CA3 damage disrupts both recent and remote episodic memories. eLife *9*, e41836. https://doi.org/10.7554/eLife.41836.
32. Salanova, V., Markand, O., and Worth, R. (2004). Temporal lobe epilepsy: analysis of patients with dual pathology. Acta Neurol. Scand. *109*, 126–131. https://doi.org/10.1034/j.1600-0404.2003.00183.x.
33. Thom, M., Eriksson, S., Martinian, L., Caboclo, L.O., McEvoy, A.W., Duncan, J.S., and Sisodiya, S.M. (2009). Temporal lobe sclerosis associated with hippocampal sclerosis in temporal lobe epilepsy: neuropathological features. J. Neuropathol. Exp. Neurol. *68*, 928–938. https://doi.org/10.1097/NEN.0b013e3181b05d67.

34. Tassi, L., Meroni, A., Deleo, F., Villani, F., Mai, R., Russo, G.L., Colombo, N., Avanzini, G., Falcone, C., Bramerio, M., et al. (2009). Temporal lobe epilepsy: neuropathological and clinical correlations in 243 surgically treated patients. Epileptic Disord. *11*, 281–292. https://doi.org/10.1684/epd.2009.0279.

35. Mitchnick, K.A., Labardo, S., and Rosenbaum, R.S. (2024). Dissociations in perceptual discrimination following selective damage to the dentate gyrus versus CA1 subfield of the hippocampus. Cortex *179*, 191–214. https://doi.org/10.1016/j.cortex.2024.06.020.

36. Baker, S., Vieweg, P., Gao, F., Gilboa, A., Wolbers, T., Black, S.E., and Rosenbaum, R.S. (2016). The Human Dentate Gyrus Plays a Necessary Role in Discriminating New Memories. Curr. Biol. *26*, 2629–2634. https://doi.org/10.1016/j.cub.2016.07.081.

37. Miller, T.D., Chong, T.T.J., Aimola Davies, A.M., Ng, T.W.C., Johnson, M.R., Irani, S.R., Vincent, A., Husain, M., Jacob, S., Maddison, P., et al. (2017). Focal CA3 hippocampal subfield atrophy following LGI1 VGKC-complex antibody limbic encephalitis. Brain *140*, 1212–1219. https://doi.org/10.1093/brain/awx070.

38. Norman, K.A., and O'Reilly, R.C. (2003). Modeling hippocampal and neocortical contributions to recognition memory: a complementary-learning-systems approach. Psychol. Rev. *110*, 611–646. https://doi.org/10.1037/0033-295X.110.4.611.

39. Rugg, M.D., and Johnson, J.D. (2015). In Handbook on the Cognitive Neuroscience of Memory, A. Duarte, M.D. Barense, and D.R. Addis, eds. (Wiley-Blackwell), pp. 84–107.

40. Barry, D.N., and Maguire, E.A. (2019). Remote Memory and the Hippocampus: A Constructive Critique. Trends Cogn. Sci. *23*, 128–142. https://doi.org/10.1016/j.tics.2018.11.005.

41. Yonelinas, A.P., Ranganath, C., Ekstrom, A.D., and Wiltgen, B.J. (2019). A contextual binding theory of episodic memory: systems consolidation reconsidered. Nat. Rev. Neurosci. *20*, 364–375. https://doi.org/10.1038/s41583-019-0150-4.

42. Dimsdale-Zucker, H. R. & Ranganath, C. in Representational Similarity Analyses, Handbook of behavioral neuroscience, Handbook of in Vivo Neural Plasticity Techniques (ed D. Manahan-Vaughan) Ch. 27, 509-525 (Elsevier, 2018).

43. Bonnici, H.M., Chadwick, M.J., Kumaran, D., Hassabis, D., Weiskopf, N., and Maguire, E.A. (2012). Multi-voxel pattern analysis in human hippocampal subfields. Front. Hum. Neurosci. *6*, 290. https://doi.org/10.3389/fnhum.2012.00290.

44. Bonnici, H.M., Chadwick, M.J., and Maguire, E.A. (2013). Representations of recent and remote autobiographical memories in hippocampal subfields. Hippocampus *23*, 849–854. https://doi.org/10.1002/hipo.22155.

45. Dalmau, J., and Rosenfeld, M.R. (2014). Autoimmune encephalitis update. Neuro Oncol. *16*, 771–778. https://doi.org/10.1093/neuonc/nou030.

46. Irani, S.R., Stagg, C.J., Schott, J.M., Rosenthal, C.R., Schneider, S.A., Pettingill, P., Pettingill, R., Waters, P., Thomas, A., Voets, N.L., et al. (2013). Faciobrachial dystonic seizures: the influence of immunotherapy on seizure control and prevention of cognitive impairment in a broadening phenotype. Brain *136*, 3151–3162. https://doi.org/10.1093/brain/awt212.

47. Irani, S.R., Alexander, S., Waters, P., Kleopa, K.A., Pettingill, P., Zuliani, L., Peles, E., Buckley, C., Lang, B., and Vincent, A. (2010). Antibodies to Kv1 potassium channel-complex proteins leucine-rich, glioma inactivated 1 protein and contactin-associated protein-2 in limbic encephalitis, Morvan's syndrome and acquired neuromyotonia. Brain *133*, 2734–2748. https://doi.org/10.1093/brain/awq213.

48. Finke, C., Prüss, H., Heine, J., Reuter, S., Kopp, U.A., Wegner, F., Then Bergh, F., Koch, S., Jansen, O., Münte, T., et al. (2017). Evaluation of Cognitive Deficits and Structural Hippocampal Damage in Encephalitis With Leucine-Rich, Glioma-Inactivated 1 Antibodies. JAMA Neurol. *74*, 50–59. https://doi.org/10.1001/jamaneurol.2016.4226.

49. McCormick, C., Rosenthal, C.R., Miller, T.D., and Maguire, E.A. (2016). Hippocampal Damage Increases Deontological Responses during Moral Decision Making. J. Neurosci. *36*, 12157–12167. https://doi.org/10.1523/JNEUROSCI.0707-16.2016.

50. McCormick, C., Rosenthal, C.R., Miller, T.D., and Maguire, E.A. (2017). Deciding what is possible and impossible following hippocampal damage in humans. Hippocampus *27*, 303–314. https://doi.org/10.1002/hipo.22694.

51. McCormick, C., Rosenthal, C.R., Miller, T.D., and Maguire, E.A. (2018). Mind-Wandering in People with Hippocampal Damage. J. Neurosci. *38*, 2745–2754. https://doi.org/10.1523/JNEUROSCI.1812-17.2018.

52. Spano, G., Pizzamiglio, G., McCormick, C., Clark, I.A., De Felice, S., Miller, T.D., Edgin, J.O., Rosenthal, C.R., and Maguire, E.A. (2020). Dreaming with hippocampal damage. eLife *9*, e56211. https://doi.org/10.7554/eLife.56211.

53. Spano, G., Weber, F.D., Pizzamiglio, G., McCormick, C., Miller, T.D., Rosenthal, C.R., Edgin, J.O., and Maguire, E.A. (2020). Sleeping with Hippocampal Damage. Curr. Biol. *30*, 523–529.e523. https://doi.org/10.1016/j.cub.2019.11.072.

54. Wagner, J., Weber, B., and Elger, C.E. (2015). Early and chronic gray matter volume changes in limbic encephalitis revealed by voxel-based morphometry. Epilepsia *56*, 754–761. https://doi.org/10.1111/epi.12968.

55. Wagner, J., Witt, J.A., Helmstaedter, C., Malter, M.P., Weber, B., and Elger, C.E. (2015). Automated volumetry of the mesiotemporal structures in antibody-associated limbic encephalitis. J. Neurol. Neurosurg. Psychiatry *86*, 735–742. https://doi.org/10.1136/jnnp-2014-307875.

56. Levine, B., Svoboda, E., Hay, J.F., Winocur, G., and Moscovitch, M. (2002). Aging and autobiographical memory: dissociating episodic from semantic retrieval. Psychol. Aging *17*, 677–689.

57. Robin, J., Rivest, J., Rosenbaum, R.S., and Moscovitch, M. (2019). Remote spatial and autobiographical memory in cases of episodic amnesia and topographical disorientation. Cortex *119*, 237–257. https://doi.org/10.1016/j.cortex.2019.04.013.

58. Grilli, M.D., and Verfaellie, M. (2015). Supporting the self-concept with memory: insight from amnesia. Soc. Cogn. Affect. Neurosci. *10*, 1684–1692. https://doi.org/10.1093/scan/nsv056.

59. Rosenbaum, R.S., Moscovitch, M., Foster, J.K., Schnyer, D.M., Gao, F., Kovacevic, N., Verfaellie, M., Black, S.E., and Levine, B. (2008). Patterns of autobiographical memory loss in medial-temporal lobe amnesic patients. J. Cogn. Neurosci. *20*, 1490–1506. https://doi.org/10.1162/jocn.2008.20105.

60. Popal, H., Wang, Y., and Olson, I.R. (2019). A Guide to Representational Similarity Analysis for Social Neuroscience. Soc. Cogn. Affect. Neurosci. *14*, 1243–1253. https://doi.org/10.1093/scan/nsz099.

61. Kriegeskorte, N., Mur, M., and Bandettini, P. (2008). Representational similarity analysis - connecting the branches of systems neuroscience. Front. Syst. Neurosci. *2*, 4. https://doi.org/10.3389/neuro.06.004.2008.

62. Kriegeskorte, N., Mur, M., Ruff, D.A., Kiani, R., Bodurka, J., Esteky, H., Tanaka, K., and Bandettini, P.A. (2008). Matching categorical object representations in inferior temporal cortex of man and monkey. Neuron *60*, 1126–1141. https://doi.org/10.1016/j.neuron.2008.10.043.

63. Chadwick, M.J., Hassabis, D., and Maguire, E.A. (2011). Decoding overlapping memories in the medial temporal lobes using high-resolution fMRI. Learn. Mem. *18*, 742–746. https://doi.org/10.1101/lm.023671.111.

64. Chadwick, M.J., Bonnici, H.M., and Maguire, E.A. (2014). CA3 size predicts the precision of memory recall. Proc. Natl. Acad. Sci. USA *111*, 10720–10725. https://doi.org/10.1073/pnas.1319641111.

65. Bonnici, H.M., Sidhu, M., Chadwick, M.J., Duncan, J.S., and Maguire, E.A. (2013). Assessing hippocampal functional reserve in temporal lobe epilepsy: a multi-voxel pattern analysis of fMRI data. Epilepsy Res. *105*, 140–149. https://doi.org/10.1016/j.eplepsyres.2013.01.004.

66. Gordon, A.M., Rissman, J., Kiani, R., and Wagner, A.D. (2014). Cortical reinstatement mediates the relationship between content-specific

encoding activity and subsequent recollection decisions. Cereb. Cortex *24*, 3350–3364. https://doi.org/10.1093/cercor/bht194.

67. Ritchey, M., Wing, E.A., LaBar, K.S., and Cabeza, R. (2013). Neural similarity between encoding and retrieval is related to memory via hippocampal interactions. Cereb. Cortex *23*, 2818–2828. https://doi.org/10.1093/cercor/bhs258.
68. Tompary, A., Duncan, K., and Davachi, L. (2016). High-resolution investigation of memory-specific reinstatement in the hippocampus and perirhinal cortex. Hippocampus *26*, 995–1007. https://doi.org/10.1002/hipo.22582.
69. St-Laurent, M., Rosenbaum, R.S., Olsen, R.K., and Buchsbaum, B.R. (2020). Representation of viewed and recalled film clips in patterns of brain activity in a person with developmental amnesia. Neuropsychologia *142*, 107436. https://doi.org/10.1016/j.neuropsychologia.2020.107436.
70. Sommer, V.R., and Sander, M.C. (2022). Contributions of representational distinctiveness and stability to memory performance and age differences. Neuropsychol. Dev. Cogn. B Aging Neuropsychol. Cogn. *29*, 443–462. https://doi.org/10.1080/13825585.2021.2019184.
71. Kluen, L.M., Dandolo, L.C., Jocham, G., and Schwabe, L. (2019). Dorsolateral Prefrontal Cortex Enables Updating of Established Memories. Cereb. Cortex *29*, 4154–4168. https://doi.org/10.1093/cercor/bhy298.
72. Blank, H., Alink, A., and Büchel, C. (2023). Multivariate functional neuroimaging analyses reveal that strength-dependent face expectations are represented in higher-level face-identity areas. Commun. Biol. *6*, 135. https://doi.org/10.1038/s42003-023-04508-8.
73. Reed, J.M., and Squire, L.R. (1997). Impaired recognition memory in patients with lesions limited to the hippocampal formation. Behav. Neurosci. *111*, 667–675. https://doi.org/10.1037//0735-7044.111.4.667.
74. Viskontas, I.V., Carr, V.A., Engel, S.A., and Knowlton, B.J. (2009). The neural correlates of recollection: hippocampal activation declines as episodic memory fades. Hippocampus *19*, 265–272. https://doi.org/10.1002/hipo.20503.
75. Manns, J.R., and Squire, L.R. (1999). Impaired recognition memory on the Doors and People Test after damage limited to the hippocampal region. Hippocampus *9*, 495–499. https://doi.org/10.1002/(SICI)1098-1063(1999)9:5<495::AID-HIPO2>3.0.CO;2-O.
76. Holdstock, J.S., Mayes, A.R., Roberts, N., Cezayirli, E., Isaac, C.L., O'Reilly, R.C., and Norman, K.A. (2002). Under what conditions is recognition spared relative to recall after selective hippocampal damage in humans? Hippocampus *12*, 341–351. https://doi.org/10.1002/hipo.10011.
77. Miller, T.D., Kennard, C., Gowland, P.A., Antoniades, C.A., and Rosenthal, C.R. (2024). Differential effects of bilateral hippocampal CA3 damage on the implicit learning and recognition of complex event sequences. Cogn. Neurosci. *15*, 27–55. https://doi.org/10.1080/17588928.2024.2315818.
78. Bakker, A., Kirwan, C.B., Miller, M., and Stark, C.E.L. (2008). Pattern separation in the human hippocampal CA3 and dentate gyrus. Science *319*, 1640–1642. https://doi.org/10.1126/science.1152882.
79. Backus, A.R., Bosch, S.E., Ekman, M., Grabovetsky, A.V., and Doeller, C.F. (2016). Mnemonic convergence in the human hippocampus. Nat. Commun. *7*, 11991. https://doi.org/10.1038/ncomms11991.
80. Crossley, N.A., Mechelli, A., Scott, J., Carletti, F., Fox, P.T., McGuire, P., and Bullmore, E.T. (2014). The hubs of the human connectome are generally implicated in the anatomy of brain disorders. Brain *137*, 2382–2395. https://doi.org/10.1093/brain/awu132.
81. Misic, B., Goni, J., Betzel, R.F., Sporns, O., and McIntosh, A.R. (2014). A network convergence zone in the hippocampus. PLoS Comput. Biol. *10*, e1003982. https://doi.org/10.1371/journal.pcbi.1003982.
82. Carrera, E., and Tononi, G. (2014). Diaschisis: past, present, future. Brain *137*, 2408–2422. https://doi.org/10.1093/brain/awu101.
83. Yassa, M.A., Lacy, J.W., Stark, S.M., Albert, M.S., Gallagher, M., and Stark, C.E.L. (2011). Pattern separation deficits associated with increased hippocampal CA3 and dentate gyrus activity in nondemented older adults. Hippocampus *21*, 968–979. https://doi.org/10.1002/hipo.20808.
84. Davachi, L., and DuBrow, S. (2015). How the hippocampus preserves order: the role of prediction and context. Trends Cogn. Sci. *19*, 92–99. https://doi.org/10.1016/j.tics.2014.12.004.
85. Berkman, E.T., and Falk, E.B. (2013). Beyond Brain Mapping: Using Neural Measures to Predict Real-World Outcomes. Curr. Dir. Psychol. Sci. *22*, 45–50. https://doi.org/10.1177/0963721412469394.
86. Pegors, T.K., Tompson, S., O'Donnell, M.B., and Falk, E.B. (2017). Predicting behavior change from persuasive messages using neural representational similarity and social network analyses. Neuroimage *157*, 118–128. https://doi.org/10.1016/j.neuroimage.2017.05.063.
87. Lee, J., and Geng, J.J. (2017). Idiosyncratic Patterns of Representational Similarity in Prefrontal Cortex Predict Attentional Performance. J. Neurosci. *37*, 1257–1268. https://doi.org/10.1523/JNEUROSCI.1407-16.2016.
88. Butler, C.R., Miller, T.D., Kaur, M.S., Baker, I.W., Boothroyd, G.D., Illman, N.A., Rosenthal, C.R., Vincent, A., and Buckley, C.J. (2014). Persistent anterograde amnesia following limbic encephalitis associated with antibodies to the voltage-gated potassium channel complex. J. Neurol. Neurosurg. Psychiatry *85*, 387–391. https://doi.org/10.1136/jnnp-2013-306724.
89. Kali, S., and Dayan, P. (2004). Off-line replay maintains declarative memories in a model of hippocampal-neocortical interactions. Nat. Neurosci. *7*, 286–294. https://doi.org/10.1038/nn1202.
90. McClelland, J.L., McNaughton, B.L., and O'Reilly, R.C. (1995). Why there are complementary learning systems in the hippocampus and neocortex: insights from the successes and failures of connectionist models of learning and memory. Psychol. Rev. *102*, 419–457. https://doi.org/10.1037/0033-295X.102.3.419.
91. Wang, S.H., and Morris, R.G.M. (2010). Hippocampal-neocortical interactions in memory formation, consolidation, and reconsolidation. Annu. Rev. Psychol. *61*, 49–79. https://doi.org/10.1146/annurev.psych.093008.100523.
92. Maguire, E.A. (2001). Neuroimaging studies of autobiographical event memory. Philos. Trans. R. Soc. Lond. B Biol. Sci. *356*, 1441–1451. https://doi.org/10.1098/rstb.2001.0944.
93. Svoboda, E., McKinnon, M.C., and Levine, B. (2006). The functional neuroanatomy of autobiographical memory: a meta-analysis. Neuropsychologia *44*, 2189–2208. https://doi.org/10.1016/j.neuropsychologia.2006.05.023.
94. Aly, M., and Turk-Browne, N.B. (2016). Attention Stabilizes Representations in the Human Hippocampus. Cereb. Cortex *26*, 783–796. https://doi.org/10.1093/cercor/bhv041.
95. Guzman, S.J., Schlögl, A., Frotscher, M., and Jonas, P. (2016). Synaptic mechanisms of pattern completion in the hippocampal CA3 network. Science *353*, 1117–1123. https://doi.org/10.1126/science.aaf1836.
96. Lee, I., Yoganarasimha, D., Rao, G., and Knierim, J.J. (2004). Comparison of population coherence of place cells in hippocampal subfields CA1 and CA3. Nature *430*, 456–459. https://doi.org/10.1038/nature02739.
97. Rolls, E.T., and Treves, A. (2024). A theory of hippocampal function: New developments. Prog. Neurobiol. *238*, 102636. https://doi.org/10.1016/j.pneurobio.2024.102636.
98. Wagner, A.D., Shannon, B.J., Kahn, I., and Buckner, R.L. (2005). Parietal lobe contributions to episodic memory retrieval. Trends Cogn. Sci. *9*, 445–453. https://doi.org/10.1016/j.tics.2005.07.001.
99. Cabeza, R., Ciaramelli, E., Olson, I.R., and Moscovitch, M. (2008). The parietal cortex and episodic memory: an attentional account. Nat. Rev. Neurosci. *9*, 613–625. https://doi.org/10.1038/nrn2459.
100. Vilberg, K.L., and Rugg, M.D. (2008). Memory retrieval and the parietal cortex: a review of evidence from a dual-process perspective.

Neuropsychologia *46*, 1787–1799. https://doi.org/10.1016/j.neuropsychologia.2008.01.004.

101. Rugg, M.D., and King, D.R. (2018). Ventral lateral parietal cortex and episodic memory retrieval. Cortex *107*, 238–250. https://doi.org/10.1016/j.cortex.2017.07.012.
102. Seghier, M.L. (2013). The angular gyrus: multiple functions and multiple subdivisions. Neuroscientist *19*, 43–61. https://doi.org/10.1177/1073858412440596.
103. Bellana, B., Liu, Z., Anderson, J.A.E., Moscovitch, M., and Grady, C.L. (2016). Laterality effects in functional connectivity of the angular gyrus during rest and episodic retrieval. Neuropsychologia *80*, 24–34. https://doi.org/10.1016/j.neuropsychologia.2015.11.004.
104. Andrews-Hanna, J.R., Reidler, J.S., Sepulcre, J., Poulin, R., and Buckner, R.L. (2010). Functional-anatomic fractionation of the brain's default network. Neuron *65*, 550–562. https://doi.org/10.1016/j.neuron.2010.02.005.
105. Flegal, K.E., Marín-Gutiérrez, A., Ragland, J.D., and Ranganath, C. (2014). Brain mechanisms of successful recognition through retrieval of semantic context. J. Cogn. Neurosci. *26*, 1694–1704. https://doi.org/10.1162/jocn_a_00587.
106. Bonnici, H.M., Cheke, L.G., Green, D.A.E., FitzGerald, T.H.M.B., and Simons, J.S. (2018). Specifying a Causal Role for Angular Gyrus in Autobiographical Memory. J. Neurosci. *38*, 10438–10443. https://doi.org/10.1523/JNEUROSCI.1239-18.2018.
107. White, T.P., Engen, N.H., Sørensen, S., Overgaard, M., and Shergill, S.S. (2014). Uncertainty and confidence from the triple-network perspective: voxel-based meta-analyses. Brain Cogn. *85*, 191–200. https://doi.org/10.1016/j.bandc.2013.12.002.
108. Kwok, S.C., Shallice, T., and Macaluso, E. (2012). Functional anatomy of temporal organisation and domain-specificity of episodic memory retrieval. Neuropsychologia *50*, 2943–2955. https://doi.org/10.1016/j.neuropsychologia.2012.07.025.
109. Markowitsch, H.J. (1995). Which brain regions are critically involved in the retrieval of old episodic memory? Brain Res. Brain Res. Rev. *21*, 117–127. https://doi.org/10.1016/0165-0173(95)00007-0.
110. Daviddi, S., Pedale, T., St Jacques, P.L., Schacter, D.L., and Santangelo, V. (2023). Common and distinct correlates of construction and elaboration of episodic-autobiographical memory: An ALE meta-analysis. Cortex *163*, 123–138. https://doi.org/10.1016/j.cortex.2023.03.005.
111. Peters, S.L., and Sheldon, S. (2021). Common and distinct neural systems support the generation retrieval phase of autobiographical memory and personal problem solving. Behav. Brain Res. *397*, 112911. https://doi.org/10.1016/j.bbr.2020.112911.
112. Greenberg, D.L., Rice, H.J., Cooper, J.J., Cabeza, R., Rubin, D.C., and Labar, K.S. (2005). Co-activation of the amygdala, hippocampus and inferior frontal gyrus during autobiographical memory retrieval. Neuropsychologia *43*, 659–674. https://doi.org/10.1016/j.neuropsychologia.2004.09.002.
113. Denkova, E., Dolcos, S., and Dolcos, F. (2013). The Effect of Retrieval Focus and Emotional Valence on the Inferior Frontal Cortex Activity during Autobiographical Recollection. Front. Behav. Neurosci. *7*, 192. https://doi.org/10.3389/fnbeh.2013.00192.
114. Cabeza, R., Locantore, J.K., and Anderson, N.D. (2003). Lateralization of prefrontal activity during episodic memory retrieval: evidence for the production-monitoring hypothesis. J. Cogn. Neurosci. *15*, 249–259. https://doi.org/10.1162/089892903321208187.
115. Dobbins, I.G., and Wagner, A.D. (2005). Domain-general and domain-sensitive prefrontal mechanisms for recollecting events and detecting novelty. Cereb. Cortex *15*, 1768–1778. https://doi.org/10.1093/cercor/bhi054.
116. Badre, D., and D'Esposito, M. (2009). Is the rostro-caudal axis of the frontal lobe hierarchical? Nat. Rev. Neurosci. *10*, 659–669. https://doi.org/10.1038/nrn2667.
117. Fletcher, P.C., Shallice, T., Frith, C.D., Frackowiak, R.S., and Dolan, R.J. (1998). The functional roles of prefrontal cortex in episodic memory. II. Retrieval. Brain *121*, 1249–1256. https://doi.org/10.1093/brain/121.7.1249.
118. Badre, D. (2008). Cognitive control, hierarchy, and the rostro-caudal organization of the frontal lobes. Trends Cogn. Sci. *12*, 193–200. https://doi.org/10.1016/j.tics.2008.02.004.
119. Koechlin, E., Ody, C., and Kouneiher, F. (2003). The architecture of cognitive control in the human prefrontal cortex. Science *302*, 1181–1185. https://doi.org/10.1126/science.1088545.
120. Kuhl, B.A., Kahn, I., Dudukovic, N.M., and Wagner, A.D. (2008). Overcoming suppression in order to remember: contributions from anterior cingulate and ventrolateral prefrontal cortex. Cogn. Affect. Behav. Neurosci. *8*, 211–221. https://doi.org/10.3758/cabn.8.2.211.
121. Henson, R.N., Shallice, T., and Dolan, R.J. (1999). Right prefrontal cortex and episodic memory retrieval: a functional MRI test of the monitoring hypothesis. Brain *122*, 1367–1381. https://doi.org/10.1093/brain/122.7.1367.
122. Ranganath, C., Heller, A., Cohen, M.X., Brozinsky, C.J., and Rissman, J. (2005). Functional connectivity with the hippocampus during successful memory formation. Hippocampus *15*, 997–1005. https://doi.org/10.1002/hipo.20141.
123. Frey, S., and Petrides, M. (2000). Orbitofrontal cortex: A key prefrontal region for encoding information. Proc. Natl. Acad. Sci. USA *97*, 8723–8727. https://doi.org/10.1073/pnas.140543497.
124. Frey, S., and Petrides, M. (2002). Orbitofrontal cortex and memory formation. Neuron *36*, 171–176. https://doi.org/10.1016/s0896-6273(02)00901-7.
125. Duarte, A., Henson, R.N., Knight, R.T., Emery, T., and Graham, K.S. (2010). Orbito-frontal cortex is necessary for temporal context memory. J. Cogn. Neurosci. *22*, 1819–1831. https://doi.org/10.1162/jocn.2009.21316.
126. Stieger, J.R., Pinheiro-Chagas, P., Fang, Y., Li, J., Lusk, Z., Perry, C.M., Girn, M., Contreras, D., Chen, Q., Huguenard, J.R., et al. (2024). Cross-regional coordination of activity in the human brain during autobiographical self-referential processing. Proc. Natl. Acad. Sci. USA *121*, e2316021121. https://doi.org/10.1073/pnas.2316021121.
127. Eichenbaum, H. (2017). Time (and space) in the hippocampus. Curr. Opin. Behav. Sci. *17*, 65–70. https://doi.org/10.1016/j.cobeha.2017.06.010.
128. Navawongse, R., and Eichenbaum, H. (2013). Distinct pathways for rule-based retrieval and spatial mapping of memory representations in hippocampal neurons. J. Neurosci. *33*, 1002–1013. https://doi.org/10.1523/JNEUROSCI.3891-12.2013.
129. Wikenheiser, A.M., Marrero-Garcia, Y., and Schoenbaum, G. (2017). Suppression of Ventral Hippocampal Output Impairs Integrated Orbitofrontal Encoding of Task Structure. Neuron *95*, 1197–1207.e3. https://doi.org/10.1016/j.neuron.2017.08.003.
130. Zhou, J., Montesinos-Cartagena, M., Wikenheiser, A.M., Gardner, M.P.H., Niv, Y., and Schoenbaum, G. (2019). Complementary Task Structure Representations in Hippocampus and Orbitofrontal Cortex during an Odor Sequence Task. Curr. Biol. *29*, 3402–3409.e3. https://doi.org/10.1016/j.cub.2019.08.040.
131. Mizrak, E., Bouffard, N.R., Libby, L.A., Boorman, E.D., and Ranganath, C. (2021). The hippocampus and orbitofrontal cortex jointly represent task structure during memory-guided decision making. Cell Rep. *37*, 110065. https://doi.org/10.1016/j.celrep.2021.110065.
132. Schnider, A., and Ptak, R. (1999). Spontaneous confabulators fail to suppress currently irrelevant memory traces. Nat. Neurosci. *2*, 677–681. https://doi.org/10.1038/10236.
133. Dalla Barba, G., Brazzarola, M., Barbera, C., Marangoni, S., Causin, F., Bartolomeo, P., and Thiebaut de Schotten, M. (2018). Different patterns of confabulation in left visuo-spatial neglect. Exp. Brain Res. *236*, 2037–2046. https://doi.org/10.1007/s00221-018-5281-8.

134. Dalla Barba, G. (1993). Different patterns of confabulation. Cortex *29*, 567–581. https://doi.org/10.1016/s0010-9452(13)80281-x.

135. Hebscher, M., Barkan-Abramski, M., Goldsmith, M., Aharon-Peretz, J., and Gilboa, A. (2016). Memory, Decision-Making, and the Ventromedial Prefrontal Cortex (vmPFC): The Roles of Subcallosal and Posterior Orbitofrontal Cortices in Monitoring and Control Processes. Cereb. Cortex *26*, 4590–4601. https://doi.org/10.1093/cercor/bhv220.

136. Duncan, J. (2010). The multiple-demand (MD) system of the primate brain: mental programs for intelligent behaviour. Trends Cogn. Sci. *14*, 172–179. https://doi.org/10.1016/j.tics.2010.01.004.

137. Yeo, B.T.T., Krienen, F.M., Sepulcre, J., Sabuncu, M.R., Lashkari, D., Hollinshead, M., Roffman, J.L., Smoller, J.W., Zöllei, L., Polimeni, J.R., et al. (2011). The organization of the human cerebral cortex estimated by intrinsic functional connectivity. J. Neurophysiol. *106*, 1125–1165. https://doi.org/10.1152/jn.00338.2011.

138. Dixon, M.L., De La Vega, A., Mills, C., Andrews-Hanna, J., Spreng, R.N., Cole, M.W., and Christoff, K. (2018). Heterogeneity within the frontoparietal control network and its relationship to the default and dorsal attention networks. Proc. Natl. Acad. Sci. USA *115*, E1598–E1607. https://doi.org/10.1073/pnas.1715766115.

139. Spreng, R.N., Sepulcre, J., Turner, G.R., Stevens, W.D., and Schacter, D.L. (2013). Intrinsic architecture underlying the relations among the default, dorsal attention, and frontoparietal control networks of the human brain. J. Cogn. Neurosci. *25*, 74–86. https://doi.org/10.1162/jocn_a_00281.

140. McCaig, R.G., Dixon, M., Keramatian, K., Liu, I., and Christoff, K. (2011). Improved modulation of rostrolateral prefrontal cortex using real-time fMRI training and meta-cognitive awareness. Neuroimage *55*, 1298–1305. https://doi.org/10.1016/j.neuroimage.2010.12.016.

141. Burgess, P.W., Dumontheil, I., and Gilbert, S.J. (2007). The gateway hypothesis of rostral prefrontal cortex (area 10) function. Trends Cogn. Sci. *11*, 290–298. https://doi.org/10.1016/j.tics.2007.05.004.

142. Fornito, A., Harrison, B.J., Zalesky, A., and Simons, J.S. (2012). Competitive and cooperative dynamics of large-scale brain functional networks supporting recollection. Proc. Natl. Acad. Sci. USA *109*, 12788–12793. https://doi.org/10.1073/pnas.1204185109.

143. Gilbert, S.J., Spengler, S., Simons, J.S., Steele, J.D., Lawrie, S.M., Frith, C.D., and Burgess, P.W. (2006). Functional specialization within rostral prefrontal cortex (area 10): a meta-analysis. J. Cogn. Neurosci. *18*, 932–948. https://doi.org/10.1162/jocn.2006.18.6.932.

144. Westphal, A.J., Wang, S., and Rissman, J. (2017). Episodic Memory Retrieval Benefits from a Less Modular Brain Network Organization. J. Neurosci. *37*, 3523–3531. https://doi.org/10.1523/JNEUROSCI.2509-16.2017.

145. Buckner, R.L., Andrews-Hanna, J.R., and Schacter, D.L. (2008). The brain's default network: anatomy, function, and relevance to disease. Ann. N. Y. Acad. Sci. *1124*, 1–38. https://doi.org/10.1196/annals.1440.011.

146. Andrews-Hanna, J.R., Saxe, R., and Yarkoni, T. (2014). Contributions of episodic retrieval and mentalizing to autobiographical thought: evidence from functional neuroimaging, resting-state connectivity, and fMRI meta-analyses. Neuroimage *91*, 324–335. https://doi.org/10.1016/j.neuroimage.2014.01.032.

147. Konishi, M., McLaren, D.G., Engen, H., and Smallwood, J. (2015). Shaped by the Past: The Default Mode Network Supports Cognition that Is Independent of Immediate Perceptual Input. PLoS One *10*, e0132209. https://doi.org/10.1371/journal.pone.0132209.

148. Stokes, M.G., Kusunoki, M., Sigala, N., Nili, H., Gaffan, D., and Duncan, J. (2013). Dynamic coding for cognitive control in prefrontal cortex. Neuron *78*, 364–375. https://doi.org/10.1016/j.neuron.2013.01.039.

149. Dixon, M.L., and Christoff, K. (2012). The decision to engage cognitive control is driven by expected reward-value: neural and behavioral evidence. PLoS One *7*, e51637. https://doi.org/10.1371/journal.pone.0051637.

150. Bunge, S.A., Kahn, I., Wallis, J.D., Miller, E.K., and Wagner, A.D. (2003). Neural circuits subserving the retrieval and maintenance of abstract rules. J. Neurophysiol. *90*, 3419–3428. https://doi.org/10.1152/jn.00910.2002.

151. Cole, M.W., Bagic, A., Kass, R., and Schneider, W. (2010). Prefrontal dynamics underlying rapid instructed task learning reverse with practice. J. Neurosci. *30*, 14245–14254. https://doi.org/10.1523/JNEUROSCI.1662-10.2010.

152. Baldauf, D., and Desimone, R. (2014). Neural mechanisms of object-based attention. Science *344*, 424–427. https://doi.org/10.1126/science.1247003.

153. Bichot, N.P., Heard, M.T., DeGennaro, E.M., and Desimone, R. (2015). A Source for Feature-Based Attention in the Prefrontal Cortex. Neuron *88*, 832–844. https://doi.org/10.1016/j.neuron.2015.10.001.

154. Dalton, M.A., Zeidman, P., McCormick, C., and Maguire, E.A. (2018). Differentiable Processing of Objects, Associations, and Scenes within the Hippocampus. J. Neurosci. *38*, 8146–8159. https://doi.org/10.1523/JNEUROSCI.0263-18.2018.

155. Squire, L.R., and Alvarez, P. (1995). Retrograde amnesia and memory consolidation: a neurobiological perspective. Curr. Opin. Neurobiol. *5*, 169–177. https://doi.org/10.1016/0959-4388(95)80023-9.

156. Mullally, S.L., Hassabis, D., and Maguire, E.A. (2012). Scene construction in amnesia: an FMRI study. J. Neurosci. *32*, 5646–5653. https://doi.org/10.1523/JNEUROSCI.5522-11.2012.

157. Barense, M.D., Ngo, J.K.W., Hung, L.H.T., and Peterson, M.A. (2012). Interactions of memory and perception in amnesia: the figure-ground perspective. Cereb. Cortex *22*, 2680–2691. https://doi.org/10.1093/cercor/bhr347.

158. Schacter, D.L., Addis, D.R., and Buckner, R.L. (2007). Remembering the past to imagine the future: the prospective brain. Nat. Rev. Neurosci. *8*, 657–661. https://doi.org/10.1038/nrn2213.

159. Beer, J.S., Lombardo, M.V., and Bhanji, J.P. (2010). Roles of medial prefrontal cortex and orbitofrontal cortex in self-evaluation. J. Cogn. Neurosci. *22*, 2108–2119. https://doi.org/10.1162/jocn.2009.21359.

160. Northoff, G., Heinzel, A., de Greck, M., Bermpohl, F., Dobrowolny, H., and Panksepp, J. (2006). Self-referential processing in our brain–a meta-analysis of imaging studies on the self. Neuroimage *31*, 440–457. https://doi.org/10.1016/j.neuroimage.2005.12.002.

161. Philippi, C.L., Duff, M.C., Denburg, N.L., Tranel, D., and Rudrauf, D. (2012). Medial PFC damage abolishes the self-reference effect. J. Cogn. Neurosci. *24*, 475–481. https://doi.org/10.1162/jocn_a_00138.

162. Gilboa, A., Winocur, G., Grady, C.L., Hevenor, S.J., and Moscovitch, M. (2004). Remembering our past: functional neuroanatomy of recollection of recent and very remote personal events. Cereb. Cortex *14*, 1214–1225. https://doi.org/10.1093/cercor/bhh082.

163. Lin, W.J., Horner, A.J., and Burgess, N. (2016). Ventromedial prefrontal cortex, adding value to autobiographical memories. Sci. Rep. *6*, 28630. https://doi.org/10.1038/srep28630.

164. Moscovitch, M. (1992). Memory and Working-with-Memory: A Component Process Model Based on Modules and Central Systems. J. Cogn. Neurosci. *4*, 257–267. https://doi.org/10.1162/jocn.1992.4.3.257.

165. Moscovitch, M., and Winocur, G. (2002). In Principles of Frontal Lobe Function, D.T. Stuss and R.T. Knight, eds. (OxfordUniversity Press), pp. 188–209.

166. Shallice, T., and Burgess, P. (1996). The domain of supervisory processes and temporal organization of behaviour. Philos. Trans. R. Soc. Lond. B Biol. Sci. *351*, 1405–1412, discussion 1411-1402. https://doi.org/10.1098/rstb.1996.0124.

167. McCormick, C., Ciaramelli, E., De Luca, F., and Maguire, E.A. (2018). Comparing and Contrasting the Cognitive Effects of Hippocampal and Ventromedial Prefrontal Cortex Damage: A Review of Human Lesion

Studies. Neuroscience *374*, 295–318. https://doi.org/10.1016/j.neuroscience.2017.07.066.

168. McCormick, C., Barry, D.N., Jafarian, A., Barnes, G.R., and Maguire, E.A. (2020). vmPFC Drives Hippocampal Processing during Autobiographical Memory Recall Regardless of Remoteness. Cereb. Cortex *30*, 5972–5987. https://doi.org/10.1093/cercor/bhaa172.
169. Gilboa, A., and Marlatte, H. (2017). Neurobiology of Schemas and Schema-Mediated Memory. Trends Cogn. Sci. *21*, 618–631. https://doi.org/10.1016/j.tics.2017.04.013.
170. Winocur, G., Moscovitch, M., and Bontempi, B. (2010). Memory formation and long-term retention in humans and animals: convergence towards a transformation account of hippocampal-neocortical interactions. Neuropsychologia *48*, 2339–2356. https://doi.org/10.1016/j.neuropsychologia.2010.04.016.
171. Winocur, G., and Weiskranitz, L. (1976). An investigation of paired-associate learning in amnesic patients. Neuropsychologia *14*, 97–110. https://doi.org/10.1016/0028-3932(76)90011-7.
172. Warrington, E., and Weiskranitz, L. (1974). The effect of prior learning on subsequent retention in amnestic patients. Neuropsychologia *12*, 419–428. https://doi.org/10.1016/0028-3932(74)90072-4.
173. Cowan, N., Beschin, N., and Della Sala, S. (2004). Verbal recall in amnesiacs under conditions of diminished retroactive interference. Brain *127*, 825–834. https://doi.org/10.1093/brain/awh107.
174. Dewar, M.T., Cowan, N., and Sala, S.D. (2007). Forgetting due to retroactive interference: a fusion of Muller and Pilzecker's (1900) early insights into everyday forgetting and recent research on anterograde amnesia. Cortex *43*, 616–634. https://doi.org/10.1016/s0010-9452(08)70492-1.
175. Dewar, M., Garcia, Y.F., Cowan, N., and Della Sala, S. (2009). Delaying interference enhances memory consolidation in amnesic patients. Neuropsychology *23*, 627–634. https://doi.org/10.1037/a0015568.
176. Barnes, C.A., Suster, M.S., Shen, J., and McNaughton, B.L. (1997). Multistability of cognitive maps in the hippocampus of old rats. Nature *388*, 272–275. https://doi.org/10.1038/40859.
177. Schimanski, L.A., Lipa, P., and Barnes, C.A. (2013). Tracking the course of hippocampal representations during learning: when is the map required? J. Neurosci. *33*, 3094–3106. https://doi.org/10.1523/JNEUROSCI.1348-12.2013.
178. Barnes, C.A. (1994). Normal aging: regionally specific changes in hippocampal synaptic transmission. Trends Neurosci. *17*, 13–18. https://doi.org/10.1016/0166-2236(94)90029-9.
179. Hayashi, Y., Kobayakawa, K., and Kobayakawa, R. (2023). The temporal and contextual stability of activity levels in hippocampal CA1 cells. Proc. Natl. Acad. Sci. USA *120*, e2221141120. https://doi.org/10.1073/pnas.2221141120.
180. Zheng, L., Gao, Z., Doner, S., Oyao, A., Forloines, M., Grilli, M.D., Barnes, C.A., and Ekstrom, A.D. (2023). Hippocampal contributions to novel spatial learning are both age-related and age-invariant. Proc. Natl. Acad. Sci. USA *120*, e2307884120. https://doi.org/10.1073/pnas.2307884120.
181. Buzsaki, G., and Moser, E.I. (2013). Memory, navigation and theta rhythm in the hippocampal-entorhinal system. Nat. Neurosci. *16*, 130–138. https://doi.org/10.1038/nn.3304.
182. Wilson, I.A., Ikonen, S., Gurevicius, K., McMahan, R.W., Gallagher, M., Eichenbaum, H., and Tanila, H. (2005). Place cells of aged rats in two visually identical compartments. Neurobiol. Aging *26*, 1099–1106. https://doi.org/10.1016/j.neurobiolaging.2004.09.006.
183. Chabrol, E., Navarro, V., Provenzano, G., Cohen, I., Dinocourt, C., Rivaud-Péchoux, S., Fricker, D., Baulac, M., Miles, R., Leguern, E., and Baulac, S. (2010). Electroclinical characterization of epileptic seizures in leucine-rich, glioma-inactivated 1-deficient mice. Brain *133*, 2749–2762. https://doi.org/10.1093/brain/awq171.
184. Hanert, A., Rave, J., Granert, O., Ziegler, M., Pedersen, A., Born, J., Finke, C., and Bartsch, T. (2019). Hippocampal Dentate Gyrus Atrophy Predicts Pattern Separation Impairment in Patients with LGI1 Encephalitis. Neuroscience *400*, 120–131. https://doi.org/10.1016/j.neuroscience.2018.12.046.
185. Palombo, D.J., Bacopulos, A., Amaral, R.S.C., Olsen, R.K., Todd, R.M., Anderson, A.K., and Levine, B. (2018). Episodic autobiographical memory is associated with variation in the size of hippocampal subregions. Hippocampus *28*, 69–75. https://doi.org/10.1002/hipo.22818.
186. Barry, D.N., Clark, I.A., and Maguire, E.A. (2021). The relationship between hippocampal subfield volumes and autobiographical memory persistence. Hippocampus *31*, 362–374. https://doi.org/10.1002/hipo.23293.
187. Bartsch, T., Döhring, J., Rohr, A., Jansen, O., and Deuschl, G. (2011). CA1 neurons in the human hippocampus are critical for autobiographical memory, mental time travel, and autonoetic consciousness. Proc. Natl. Acad. Sci. USA *108*, 17562–17567. https://doi.org/10.1073/pnas.1110266108.
188. Vincent, A., Bien, C.G., Irani, S.R., and Waters, P. (2011). Autoantibodies associated with diseases of the CNS: new developments and future challenges. Lancet Neurol. *10*, 759–772. https://doi.org/10.1016/S1474-4422(11)70096-5.
189. Dimsdale-Zucker, H.R., Ritchey, M., Ekstrom, A.D., Yonelinas, A.P., and Ranganath, C. (2018). CA1 and CA3 differentially support spontaneous retrieval of episodic contexts within human hippocampal subfields. Nat. Commun. *9*, 294. https://doi.org/10.1038/s41467-017-02752-1.
190. Wang, F., and Diana, R.A. (2016). Temporal context processing within hippocampal subfields. Neuroimage *134*, 261–269. https://doi.org/10.1016/j.neuroimage.2016.03.048.
191. Stevenson, R.F., Reagh, Z.M., Chun, A.P., Murray, E.A., and Yassa, M.A. (2020). Pattern Separation and Source Memory Engage Distinct Hippocampal and Neocortical Regions during Retrieval. J. Neurosci. *40*, 843–851. https://doi.org/10.1523/JNEUROSCI.0564-19.2019.
192. Gilmore, A.W., Quach, A., Kalinowski, S.E., González-Araya, E.I., Gotts, S.J., Schacter, D.L., and Martin, A. (2021). Evidence supporting a time-limited hippocampal role in retrieving autobiographical memories. Proc. Natl. Acad. Sci. USA *118*, e2023069118. https://doi.org/10.1073/pnas.2023069118.
193. Squire, L.R., Genzel, L., Wixted, J.T., and Morris, R.G. (2015). Memory consolidation. Cold Spring Harb. Perspect. Biol. *7*, a021766. https://doi.org/10.1101/cshperspect.a021766.
194. Barry, D.N., Chadwick, M.J., and Maguire, E.A. (2018). Nonmonotonic recruitment of ventromedial prefrontal cortex during remote memory recall. PLoS Biol. *16*, e2005479. https://doi.org/10.1371/journal.pbio.2005479.
195. Irani, S.R., Michell, A.W., Lang, B., Pettingill, P., Waters, P., Johnson, M.R., Schott, J.M., Armstrong, R.J.E., S Zagami, A., Bleasel, A., et al. (2011). Faciobrachial dystonic seizures precede Lgi1 antibody limbic encephalitis. Ann. Neurol. *69*, 892–900. https://doi.org/10.1002/ana.22307.
196. Wechsler, D. (1997). Wechsler Adult Intelligence Scale. 3rd edn (The Psychological Corporation).
197. Wechsler, D. (2009). Test of Premorbid Functioning: Advanced Clinical Solutions for Us with WAIS-IV and WMS-IV (The Psychological Corporation).
198. Wechsler, D. (1997). The Wechsler Memory Scale (The Psychological Corporation).
199. Osterrieth, P. (1944). Le test de copie d'une figure complexe: contribution à l'étude de la perception et de la mémoire. Arch. Psychol. *28*, 1021–1034.
200. Warrington, E. (1984). Recognition Memory Test: Manual (NFER-Nelson).
201. Robertson, I.H., Ward, T., Ridgeway, V., and Nimmo-Smith, I. (1994). The Test of Everyday Attention (Thames Valley Test Company).
202. McKenna, P., and Warrington, E. (1983). The Graded Naming Test (NFER-Nelson).

203. Delis, D.C., Kaplan, E., and J, K. (2001). Delis-Kaplan Executive Function System (The Psychological Corporation).

204. Peirce, J., Gray, J.R., Simpson, S., MacAskill, M., Höchenberger, R., Sogo, H., Kastman, E., and Lindeløv, J.K. (2019). PsychoPy2: Experiments in behavior made easy. Behav. Res. Methods *51*, 195–203. https://doi.org/10.3758/s13428-018-01193-y.

205. Reimers, N., and Gurevych, I. (2019). Sentence-BERT: Sentence Embeddings using Siamese BERT-Networks. In Proceedings of the 2019 Conference on Empirical Methods in Natural Language Processing and the 9th International Joint Conference on Natural Language Processing (EMNLP-IJCNLP). Association for Computational Linguistics, 3982–3992. https://doi.org/10.18653/v1/D19-1410.

206. Bojanowski, P., Grave, E., Joulin, A., and Mikolov, T. (2017). Enriching Word Vectors with Subword Information. Trans. Assoc. Comput. Linguist. *5*, 135–146. https://doi.org/10.1162/tacl_a_00051.

207. Callaghan, M.F., Josephs, O., Herbst, M., Zaitsev, M., Todd, N., and Weiskopf, N. (2015). An evaluation of prospective motion correction (PMC) for high resolution quantitative MRI. Front. Neurosci. *9*, 97. https://doi.org/10.3389/fnins.2015.00097.

208. Mugler, J.P., Bao, S., Mulkern, R.V., Guttmann, C.R., Robertson, R.L., Jolesz, F.A., and Brookeman, J.R. (2000). Optimized single-slab three-dimensional spin-echo MR imaging of the brain. Radiology *216*, 891–899. https://doi.org/10.1148/radiology.216.3.r00au46891.

209. Coupe, P., Manjón, J.V., Gedamu, E., Arnold, D., Robles, M., and Collins, D.L. (2010). Robust Rician noise estimation for MR images. Med. Image Anal. *14*, 483–493. https://doi.org/10.1016/j.media.2010.03.001.

210. Manjon, J.V., Coupe, P., Buades, A., Louis Collins, D., and Robles, M. (2012). New methods for MRI denoising based on sparseness and self-similarity. Med. Image Anal. *16*, 18–27. https://doi.org/10.1016/j.media.2011.04.003.

211. Ashburner, J., and Friston, K.J. (2009). Computing average shaped tissue probability templates. Neuroimage *45*, 333–341. https://doi.org/10.1016/j.neuroimage.2008.12.008.

212. Destrieux, C., Fischl, B., Dale, A., and Halgren, E. (2010). Automatic parcellation of human cortical gyri and sulci using standard anatomical nomenclature. Neuroimage *53*, 1–15. https://doi.org/10.1016/j.neuroimage.2010.06.010.

213. Farahibozorg, S.R., Henson, R.N., and Hauk, O. (2018). Adaptive cortical parcellations for source reconstructed EEG/MEG connectomes. Neuroimage *169*, 23–45. https://doi.org/10.1016/j.neuroimage.2017.09.009.

214. Greve, D.N., and Fischl, B. (2009). Accurate and robust brain image alignment using boundary-based registration. Neuroimage *48*, 63–72. https://doi.org/10.1016/j.neuroimage.2009.06.060.

215. Yushkevich, P.A., Pluta, J.B., Wang, H., Xie, L., Ding, S.L., Gertje, E.C., Mancuso, L., Kliot, D., Das, S.R., and Wolk, D.A. (2015). Automated volumetry and regional thickness analysis of hippocampal subfields and medial temporal cortical structures in mild cognitive impairment. Hum. Brain Mapp. *36*, 258–287. https://doi.org/10.1002/hbm.22627.

216. Hickling, A.L., Clark, I.A., Wu, Y.I., and Maguire, E.A. (2024). Automated protocols for delineating human hippocampal subfields from 3 Tesla and 7 Tesla magnetic resonance imaging data. Hippocampus *34*, 302–308. https://doi.org/10.1002/hipo.23606.

217. Wang, H., Suh, J.W., Das, S.R., Pluta, J.B., Craige, C., and Yushkevich, P.A. (2013). Multi-Atlas Segmentation with Joint Label Fusion. IEEE Trans. Pattern Anal. Mach. Intell. *35*, 611–623. https://doi.org/10.1109/TPAMI.2012.143.

218. Wang, H., Das, S.R., Suh, J.W., Altinay, M., Pluta, J., Craige, V., Avants, B., and Yushkevich, P.A.; Alzheimer's Disease Neuroimaging Initiative (2011). A learning-based wrapper method to correct systematic errors in automatic image segmentation: consistently improved performance in hippocampus, cortex and brain segmentation. Neuroimage *55*, 968–985. https://doi.org/10.1016/j.neuroimage.2011.01.006.

219. Dalton, M.A., Zeidman, P., Barry, D.N., Williams, E., and Maguire, E.A. (2017). Segmenting subregions of the human hippocampus on structural magnetic resonance image scans: An illustrated tutorial. Brain Neurosci. Adv. *1*, 2398212817701448. https://doi.org/10.1177/2398212817701448.

220. Dice, L.R. (1945). Measures of the amount of ecologic association between species. Ecology *26*, 297–302.

221. Spreng, R.N., and Grady, C.L. (2010). Patterns of brain activity supporting autobiographical memory, prospection, and theory of mind, and their relationship to the default mode network. J. Cogn. Neurosci. *22*, 1112–1123. https://doi.org/10.1162/jocn.2009.21282.

222. Spreng, R.N., Mar, R.A., and Kim, A.S.N. (2009). The common neural basis of autobiographical memory, prospection, navigation, theory of mind, and the default mode: a quantitative meta-analysis. J. Cogn. Neurosci. *21*, 489–510. https://doi.org/10.1162/jocn.2008.21029.

223. St-Laurent, M., Abdi, H., Burianová, H., and Grady, C.L. (2011). Influence of aging on the neural correlates of autobiographical, episodic, and semantic memory retrieval. J. Cogn. Neurosci. *23*, 4150–4163. https://doi.org/10.1162/jocn_a_00079.

224. Nawa, N.E., and Ando, H. (2019). Effective connectivity within the ventromedial prefrontal cortex-hippocampus-amygdala network during the elaboration of emotional autobiographical memories. Neuroimage *189*, 316–328. https://doi.org/10.1016/j.neuroimage.2019.01.042.

225. Nawa, N.E., and Ando, H. (2020). Effective connectivity during autobiographical memory search. Brain Behav. *10*, e01719. https://doi.org/10.1002/brb3.1719.

226. Girn, M., Setton, R., Turner, G.R., and Spreng, R.N. (2024). The "limbic network", comprising orbitofrontal and anterior temporal cortex, is part of an extended default network: Evidence from multi-echo fMRI. Netw. Neurosci. *8*, 860–882. https://doi.org/10.1162/netn_a_00385.

227. Levy, D.A. (2012). Towards an understanding of parietal mnemonic processes: some conceptual guideposts. Front. Integr. Neurosci. *6*, 41. https://doi.org/10.3389/fnint.2012.00041.

228. Andersson, J.L., Hutton, C., Ashburner, J., Turner, R., and Friston, K. (2001). Modeling geometric deformations in EPI time series. Neuroimage *13*, 903–919. https://doi.org/10.1006/nimg.2001.0746.

229. Ashburner, J., and Friston, K.J. (2005). Unified segmentation. Neuroimage *26*, 839–851. https://doi.org/10.1016/j.neuroimage.2005.02.018.

230. Mumford, J.A., Turner, B.O., Ashby, F.G., and Poldrack, R.A. (2012). Deconvolving BOLD activation in event-related designs for multivoxel pattern classification analyses. Neuroimage *59*, 2636–2643. https://doi.org/10.1016/j.neuroimage.2011.08.076.

231. Walther, A., Nili, H., Ejaz, N., Alink, A., Kriegeskorte, N., and Diedrichsen, J. (2016). Reliability of dissimilarity measures for multi-voxel pattern analysis. Neuroimage *137*, 188–200. https://doi.org/10.1016/j.neuroimage.2015.12.012.

232. Henriksson, L., Khaligh-Razavi, S.M., Kay, K., and Kriegeskorte, N. (2015). Visual representations are dominated by intrinsic fluctuations correlated between areas. Neuroimage *114*, 275–286. https://doi.org/10.1016/j.neuroimage.2015.04.026.

STAR★METHODS

KEY RESOURCES TABLE

REAGENT or RESOURCE	SOURCE	IDENTIFIER
Experimental models: Organisms/strains		
Human: patients with LGI1-LE	1) National Hospital for Neurology and Neurosurgery, UCLH NHS Trust 2) Oxford University Hospitals NHS Foundation Trust 3) King's College Hospital NHS Foundation Trust	NA
Human: control	Local advertisement/friends and family	NA
Software and algorithms		
MATLAB R2021b	MathWorks	RRID:SCR_001622, https://www.mathworks.com/
PsychoPy-2022-1.4.	PsychoPy[169]	RRID:SCR_006571, https://www.psychopy.org/
RSA Toolbox	MRC Cognition and Brain Sciences Unit, Cambridge[61]	RRID:SCR_019029, http://www.mrc-cbu.cam.ac.uk/methods-and-resources/toolboxes/license/
SPM 12	Functional Imaging Laboratory, London, UK	RRID:SCR_007037, http://fil.ion.ucl.ac.uk/spm/software/spm12/
FreeSurfer 7.3.2	Martinos Center for Biomedical Imaging, Harvard, USA[175]	RRID:SCR_001847, http://surfer.nmr.mgh.harvard.edu/
ASHS	Penn Image Computing and Science Laboratory, Philadelphia[178]	RRID: SCR_005996, https://sites.google.com/view/ashs-dox/home
SPSS version 29.0	IBM Corp	RRID:SCR_002865, https://www.ibm.com/products/spss-statistics
SBERT Sentence Textual Similarity	sbert.net	https://sbert.net/docs/sentence_transformer/pretrained_models.html
Other		
3.0-Tesla MRI Prisma scanner	Siemens	https://www.siemens-healthineers.com/magnetic-resonance-imaging/3t-mri-scanner/magnetom-prisma
JVC DLA-SX21 projector	JVC	http://pro.jvc.com/prof/attributes/tech_desc.jsp?model_id=MDL101416&feature_id=02
Etymotic Ear-Tone stereo sound system	Etymotic	https://etymotic.com/medical-devices/

EXPERIMENTAL MODEL AND SUBJECT DETAILS

Participant details

All participants in the group with hippocampal amnesia had chronic amnesia induced by a single-aetiology: leucine-rich glycine-inactivated-1 limbic encephalitis (LGI1- LE).[195] All participants were seizure-free at the time of testing and considered clinically stable by their treating neurologist (TM, MZ, AH, TP, EC). The group with hippocampal amnesia was comprised of 18 participants (mean and S.E.M. age: 58.1 ± 2.33 years, male = 13). Eighteen healthy age- and education-matched controls were recruited (58.1 ± 2.33 years, male = 13) to the control group. These control participants had no history of cognitive, psychiatric, or neurological illness. All participants had normal or corrected-to-normal vision. All participants were fluent, native English speakers. No significant differences were found between the groups in terms of age or years-of-education. LGI1-LE is a typically monophasic illness with no ongoing change in postmorbid cognition expected.[31,37,88]; Accordingly, none of the participants with amnesia had clinical evidence of a relapse at any time surrounding the experimental period. All participants with amnesia were otherwise self-reported as healthy, with no evidence of secondary gain or active psychopathology. Informed written consent was obtained from all participants for all procedures and for

consent to publish, in accordance with the terms of approval granted by a national research ethics committee (22/NW/0088) and the principles expressed in the Declaration of Helsinki. Care was taken to ensure that all aspects of this experiment (including task design, administration, and task comprehension) were undertaken to provide maximal retrieval support and facilitate task comprehension in both groups.

METHOD DETAILS

Neuropsychological assessment

Neuropsychological assessment was conducted in both groups using the following standardised neuropsychological subtests: *Verbal and visual intelligence:* Wechsler Abbreviated Scale of Intelligence (WASI) – Similarities and Matrix Reasoning;[196] *Premorbid intelligence:* Test of Premorbid Functioning – UK Version;[197] *Verbal memory:* Logical memory I and II from Wechsler Memory Scale–III (WMS-III);[198] *Visual memory:* Rey complex figure – Immediate-Recall and Delayed-Recall;[199] *Recognition memory*: Recognition Memory Test – Words and Faces;[200] *Sustained Attention*: Test of Everyday Attention – Map Search;[201] *Language*: Graded Naming Test[202]; Letter Fluency and Category Fluency from the Verbal Fluency from Delis-Kaplan Executive Function System (D-KEFS);[203] *Executive function:* Category Switching from the Verbal Fluency Test, Number-Letter Switching from the Trail Making Test from Delis-Kaplan Executive Function System (D-KEFS)[203]; and, WMS-III – Digit Span;[198] *Attentional Switching/Cognitive Flexibility:* Visual Elevator from Test of Everyday Attention[201]; and, Number-Letter Switching from the Trail Making Test from the Delis-Kaplan Executive Function System (D-KEFS);[203] *Visuomotor skills:* Visual Scanning, Number Sequencing, Letter Sequencing, and Motor Speed from the Trail Making Test from Delis-Kaplan Executive Function System (D-KEFS)[203] and *Visuoconstruction skills*: Rey complex figure – Copy.[199] Scores on the standardised neuropsychological tests were first transformed into age-corrected standard values, where available, and then transformed into *Z*-scores. One participant in the group with hippocampal amnesia was unable to complete the premorbid IQ (TOPF) test due to severe dyslexia.

Neuropsychology statistical analyses

The data from the neuropsychological assessments were analyzed in two ways: (1) two-sample *t*-tests (two-tailed) conducted to determine whether the group with hippocampal amnesia performance was significantly different from normative data (with a mean of 0 and standard deviation of 0.3); and, (2) a between-groups independent-sample *t* test (two-tailed) to determine where group level performance was significantly different between the two experimental groups.

Autobiographical interview

LGI1-LE is a discrete, autoimmune condition with reliably identifiable symptom-onset; therefore, we were able to acquire specific autobiographical memories that occurred ∼ five years before the onset of the illness, a period where autobiographical memories are hypothesised to become consolidated across the autobiographical memory network.[12,44,192–194] The monophasic nature of autoimmune encephalitis suggests that hippocampal function was intact in these participants during the encoding of memories before the disease onset. Impaired retrograde memory, therefore, probably reflects the disruption of hippocampal-mediated retrieval mechanisms rather than anterograde difficulties with encoding and consolidation. Memories were obtained from the 18 participants in the group with hippocampal amnesia and 18 participants in the control group 14 days prior to the scanning (group with hippocampal amnesia mean: 14.9 days ± 0.86, range: 13–28 days; control group mean: 16.1 days ± 3.21, range: 13–62; U = 157, p = 0.888). Episodic memories were sampled from a mean period of 5.28 ± 0.51 years before symptom onset (range: 2011–2020) in the group with hippocampal amnesia. The control group were matched to this premorbid time period (mean period of 5.50 ± 0.42 years before the group with hippocampal amnesia symptoms onset; range: 2012–2020). No between-group differences were found in the absolute age of these memories (group with hippocampal amnesia median: 5 years; controls median: 5; U = 177, p = 0.630). All participants were instructed to select three memories that were orthogonal to each other in terms of the content related to the people involved, the places, and the events to ensure they did not include any overlapping mnemonic details. All memories were checked at the point of acquisition for this degree of orthogonalisation for all participants, with no memories being rejected on the basis of these criteria. All memories provided by the individuals with amnesia were checked with family members or friends present at the time of testing, wherever possible. Episodic and semantic details associated with each of the three autobiographical memories were assessed under the retrieval conditions of the Autobiographical Interview procedure.[56] Unique cue words agreed by the experimenter and participant served as the basis for retrieval during the fMRI scan portion of the experiment.

Scoring and reliability

All verbal responses on the AI procedure were recorded in a digital audio format and then transcribed for scoring offline. Transcripts were compiled so that identifying personal details or anything that pertained to group membership were removed. Responses were scored according to the standardised method outlined in the AI Scoring Manual.[56] Accounts were segmented into informational bits/details, or those occurrences, observations, or thoughts expressed as a grammatical clause. Details that related directly to a unique event, and which had a specific time and place or were associated with episodic re-experiencing (such as thoughts or emotions), were classified as internal (episodic) details. Information that did not relate to the event was assigned to external details, and then

sub-categorized into semantic (factual information or extended events), repetitions (where previous details had been given with no new elaboration), and other (e.g., metacognitive statements, editorializing, and inferences).

One rater scored 100% of the episodes acquired, with another rater scoring 50% of the acquired episodes (including post-scan debrief; see below), which is in line with prior studies.[52,56] Intra-class correlation coefficients (ICCs) were used to calculate the agreement between the twice-repeated scoring of data acquired on the AI. A two-way mixed-model design was used to test the degree of absolute agreement, with the intraclass correlation coefficient of 0.94 indicating a high-level of consistency in scoring.

Autobiographical interview statistical analysis

In line with previous work,[31,37] we analyzed the internal (episodic) and external (semantic) points generated per participant with an omnibus ANOVA and followed up with planned comparisons. The alpha criterion was corrected for multiple comparisons using the Bonferroni-Holm procedure.

Stimuli and experimental paradigm

Task and procedure

The neuroimaging section of the experiment consisted of four parts: a pre-scan training session; an intra-scan training session; the autobiographical retrieval session; and a post-scan debriefing session. Experimental tasks were run on a Dell 15-inch laptop using PsychoPy software (v.2022.2.4.),[204] with stimulus presentation delivered via an MRI-compatible projection system (JVC DLA-SX21 projector via HDMI cables; 1400 × 1050 pixels resolution run at native resolution and a native refresh rate of 60Hz). All task stimuli were viewed on a 26 × 19.5cm screen positioned at a distance of 62cm from the participant. Tones were played through an Etymotic Ear-Tone stereo sound system.

Pre-scan training

All participants underwent training in a behavioral testing room located outside of the MRI scan room. Each pre-scan training session comprised three runs. Training runs were based on two other memories acquired during the autobiographical memory acquisition phase and conducted two-weeks prior to the scan session. On the first training run, participants were presented with the title of a retrieval cue for a specific memory. Each cue appeared on a computer screen for three seconds and was followed by the presentation of an on-screen instruction to 'Close your eyes' (12 s). Participants were instructed to close their eyes as soon as they knew which memory they had to remember and then verbally recount the memory with as much vivid detail as possible until a tone sounded. The prompt to remember and recount each episodic memory was repeated three times and in a pseudorandom order, such that each retrieval cue prompt was not presented twice in succession. The participants then had a rest screen for five-seconds before the next trial. The second training run comprised the same three memories, with each remembered three times out loud over the 15s total retrieval period. On the second run, after recounting the memory, participants were additionally asked to indicate the vividness associated with each specific memory on a four-point scale (1 – very vivid, as if like real life, 2 – vivid, but not like real life, 3 – some recollection, and 4 – no meaningful experience of the memory). Participants were asked to provide the rating within a three-second interval. After each rating, participants were then provided with a five-second rest period before the next trial. The third training run consisted of the same three practice memories with vividness ratings, each retrieved verbally three times, with the addition of a control task that was psuedorandomly interleaved with the remember trials. On the control task, participants were instructed to count up from a given starting number in a stated interval and continue counting for 15s. After each control trial, the participants were asked to rate their level of task engagement on a four-point scale (1 – entirely engaged with counting, 2 – mostly engaged with counting, 3 – some counting, and 4 – completely distracted).

During the final training run, participants were first provided with a reminder about their chosen memories and the titles associated with each memory. During this training block, participants were presented with the titles as retrieval cues for their experimental memories. All participants were encouraged to begin memory retrieval during that cue screen as detailed above, except this time all participants were asked to retrieve their memories with as much visual detail as possible and to remember silently. All the participants were able to retrieve their specific memories. Total retrieval time was once again 15s for each memory. These memories were psuedorandomly interleaved with the counting task. Both trial types were followed by their respective rating assessment and then a five-second rest period.

Intra-scan training

All participants underwent a final training session on the autobiographical memory remembering task once insider the MRI scanner. During this final training phase, participants were asked to remember each autobiographical memory in silence with their eyes closed for the three recollections in order to align with the upcoming experimental conditions. This was used to familiarise all participants to the conditions of fMRI phase of the experiment. At the end of each trial, participants were asked to provide ratings for the memory and counting trials, as detailed above, and input their numerical response via an MRI-compatible button box.

Autobiographical memory task

During the acquisition of fMRI data, participants underwent three trial runs in which each memory retrieval cue was presented five-times per block, interleaved with the counting task. The presentation of each stimulus was pseudo-randomised such that each condition was not presented in succession. In total, there were 15 trials for each memory, totalling 45 memory trials performed under fMRI conditions.

Post-scan debriefing session

At the end of the fMRI scan session, each participant underwent another recorded Autobiographical Interview procedure, where they were asked to remember what they were visualising for each memory, in as much detail as possible, on each of the memory trials. The debriefing sessions were transcribed and scored in the same manner as the Autobiographical Interview.

Semantic textual similarity analysis

To compute the semantic similarity between pre- and post-fMRI narrative texts for each experimental memory, we used a pre-trained Sentence-Bidirectional Encoder Representations from Transformers (SBERT) model, which is a modified version of the BERT architecture optimised for generating semantically meaningful sentence embeddings.[205] SBERT applies a Siamese network structure comprised of two identical BERT encoders, which independently embed each sentence into a fixed-size dense vector that captures semantic meaning. This architecture enables efficient pairwise comparisons by providing direct vector representations of individual inputs, without the need for input concatenation as would be the case for traditional BERT. Sentence embeddings generated by SBERT were then compared using cosine similarity to quantify the semantic similarity between pre- and post-scan narratives.

The pre- and post-fMRI narrative texts for each experimental memory were first preprocessed: all text was converted to lowercase for consistency, stop words were removed, and sentence boundaries (e.g., full stops) were preserved. Editorial comments or meta-textual elements were removed. Given that the intra-scan mnemonic recall period was 15s, the text of the pre-experiment memories were truncated in length to match that of the post-experiment memories. Whole paragraphs were then passed into a pre-trained SBERT model (using all-MiniLM-L6-v2) within the sentence-transformers Python library. Each narrative was embedded into a fixed-length dense vector that reflects its semantic content.

To quantify the similarity between vectors, we used cosine similarity, which quantifies the cosine of the angle between two vectors in a high-dimensional space. This metric is widely used for semantic similarity tasks because it focuses on the orientation of the vectors rather than their magnitude, making it well-suited for comparing normalised embeddings.[205,206] Cosine similarity scores, ranging from -1 (completely dissimilar) to 1 (identical), were used to compare absolute values of similarity for each memory before and after scanning between groups. Individual cosine similarity scores were generated for comparison of each pre- and post-scanning memory. These cosine similarity scores were then entered into a mixed-model omnibus ANOVA for between-group comparisons.

Data acquisition

Functional and anatomical MRI data acquisition

Structural and functional MRI data were acquired using a Siemens 3.0-Tesla Prisma MRI system (Magnetom TIM Trio, Siemens Healthcare, Erlangen, Germany) with a 64-channel head coil.

Functional MRI data were collected with a T2*-weighted echo-planar imaging (EPI) sequence (TR = 3.36s, TE = 30 ms, slice thickness = 2.5 mm, 3 $\times$ 3mm in-plane resolution, phase encoding direction = anterior $\rightarrow$ posterior, field of view = 192 mm^2, matrix size = 64 $\times$ 72, flip angle = 90°, slice tilt = -30°, 48 axial slices), resulting in total of 210 whole-brain volumes per run (lasting for $\sim$12 min per run).

A whole-brain structural T1-weighted sequence was acquired (six-minute acquisition time) after the experimental EPI runs for each participant at an isotropic resolution of 0.8mm,[207] which was used for the automated VBM analysis and FreeSurfer cortical parcellation. Whole-brain T1-weighted anatomical images consisted of 176 axial slices acquired with a magnetisation-prepared rapid gradient-echo (MPRAGE) sequence (TI = 1100 ms, TR = 2530 ms, TE = 3.34 ms, slice thickness = 1 mm, 1 mm^2 in-plane resolution, phase encoding direction = anterior $\rightarrow$ posterior, field of view = 256 mm^2, matrix size = 256 $\times$ 256, flip angle = 7°).

In order to conduct the semi-automated segmentation of the hippocampal subfields, partial volume images for the entire extent of the temporal lobes were collected using a single-slab 3D T2-weighted turbo spin-echo sequence with variable flip angles (SPACE)[208] in combination with parallel imaging to simultaneously achieve a high image resolution of $\sim$500 μm, high sampling efficiency, and short scan time while maintaining a sufficient signal-to-noise ratio (SNR). After excitation of a single axial slab, the image was readout with the following parameters: resolution = 0.5 $\times$ 0.5 $\times$ 0.5 mm, matrix = 384 $\times$ 328, partitions = 104, partition thickness = 0.5 mm, partition oversampling = 15.4%, field of view = 200 $\times$ 171 mm^2, TE = 353 ms, TR = 3200 ms, GRAPPA x 2 in phase-encoding (PE) direction, bandwidth = 434 Hz/pixel, echo spacing = 4.98 ms, turbo factor in PE direction = 177, echo train duration = 881, averages = 1.9, plane of acquisition = sagittal. To improve the SNR of the anatomical image, two scans were acquired for each participant (taking 13 min each), and then coregistered and averaged. For each participant, the 3D T2-weighted scans underwent Rician noise estimation[209] and were then denoised using oracle-based discrete cosine transform (ODCT[210]), with additional denoising then applied to the ODCT denoised image using a prefiltered rotationally invariant nonlocal means filter.[210] This computed a single denoised image for each high-resolution temporal lobe image. The denoised images were then co-registered and averaged to provide a final image for hippocampal segmentation for each participant (see below).

QUANTIFICATION AND STATISTICAL ANALYSIS

Whole-brain voxel-by-voxel morphometry and cortical parcellation

Whole-brain voxel-by-voxel morphometry (VBM) and diffeomorphic anatomical registration using the exponentiated Lie algebra (DARTEL) registration method[211] were conducted on the 3.0-Tesla (0.8 $\times$ 0.8 $\times$ 0.8mm^3 spatial resolution) T1-weighted anatomical images, using gray matter volume, white matter volume, and cerebrospinal fluid volumes as covariates. The voxel-by-voxel

contrast of normalised gray matter across the whole-brain was conducted using a two-sample *t* test thresholded at $p < 0.05$, with family-wise error correction for multiple comparisons. The results revealed no suprathreshold clusters of gray matter or white matter volume loss, nor any increase in cerebrospinal fluid volume, in the group with hippocampal amnesia relative to the control group.

T1-weighted images were also segmented and parcellated into cortical and subcortical regions of interest (ROIs) based on the Destrieux Atlas[212] using the -recon-all function in FreeSurfer version 7.3.2 (http://surfer.nmr.mgh.harvard.edu/). This atlas was chosen because it contains a greater number of cortical parcellations that correspond to the specific cytoarchitectural boundaries constituting Brodmann areas.[212] In this way, we limited the spatial extent of voxels within a given region of interest (ROI), facilitating a more fine-grained analysis.[213] Following cortical parcellation, each of the T1-weighted images obtained for each participant and the respective parcellations were transformed into the participant's native anatomical space using a rigid boundary-based registration approach, specific for registration between EPI and structural images.[214]

Anatomical segmentation of hippocampal subfields

3D T2-weighted turbo spin-echo images provided the basis for automated segmentation using the Automatic Segmentation of Hippocampal Subfields (ASHS[215]) atlas package.[216] The ASHS atlas training process works by first applying deformable coregistration of the T1-weighted image, T2-weighted image, and hippocampal subfield masks to an unbiased population template. Automatic segmentations are then produced by deformably coregistering the T2-weighted image of each participant to that of all other participants and applying joint label fusion.[217] Finally, corrective learning classifiers[218] are trained by comparing the automatic segmentations with the manual segmentation of the same T2-weighted image; see Yushkevich et al.[215] for full details of the ASHS pipeline. Once participant scans had been processed through the ASHS pipeline, all resultant hippocampal segmented images were then manually inspected and modified according to a previously described methodology[219] using the ITK Snap software (version 3.8.0). Masks were created for the following six subfields: DG/CA4, CA2/3, CA1, subiculum, pre/parasubiculum and uncus. Subfield segmentations were performed by an experienced researcher (TDM). Volumes were then corrected for intracranial volume in line with our previous work.[31,37] To evaluate intra-rater reliability, five datasets from participants in the group with hippocampal amnesia and five datasets from participants in the control group (>10% of experimental population) were re-segmented after a month had elapsed. Analyses for each subfield were conducted using the Dice overlap metric.[220] Dice scores are reported in Table S1 and ranged from 0.7259–0.9391. Intraclass correlation coefficients were derived from the 12 original and replicated subfield volumes across both segmentations (24 volumes per participant) and across both groups (240 subfield volumes in total) using a one-way random effects model.

Hippocampal subfield segmentation statistical analysis

In line with previous work,[31,37] hippocampal subfield volumes were examined using a mixed-model omnibus ANOVA and planned between-group comparisons.

Autobiographical network definition

Given the overlap between the default mode network, the autobiographical memory retrieval network,[92,93,103,126,146,221–223] and prior evidence of altered graph theoretical metrics within these regions in a cohort of individuals with amnesia secondary to LGI1-LE,[31] we sought to evaluate the RDM model fit and trial-by-trial similarity in the discrete pattern of voxels that might correspond to specific autobiographical memories within this network. Moreover, there is increasing evidence that informational components of episodic memories are supported by discrete networks, such as information about people within the anterior temporal network,[14] contextual information in the posterior medial network,[14] schema in the medial prefrontal network,[14] and event-specific representations within the hippocampus.[14] Therefore, in order to examine representational similarity within these regions, we also extended the cortical network to structures of the dorsolateral PFC (dlPFC), because the dlPFC plays a critical role within autobiographical memory retrieval,[93,110,112,121,224,225] and also appears to constitute an extended component of the default mode network.[226] Representational similarity for autobiographical memories was examined in the following regions (Destrieux Atlas labels are provided within parentheses): anterior medial prefrontal cortex (G_Orbital); posterior cingulate cortex (G_Cingul_Postdorsal); temporoparietal junction (G_occipital_middle); angular gyrus (G_parietal_inf-Angular); orbitofrontal cortex (medial and lateral; G_orbital), inferior frontal gyrus (G_Front_inf-Orbital), precuneus (G_precuneus), retrosplenial cortex (S_pericallosal), middle frontal gyrus (G_front_middle), lateral temporal cortex (G_temporal_middle), ventromedial prefrontal cortex (G_rectus), parahippocampal cortex (G_oc-temp_med-Parahip). All regions were evaluated in both hemispheres on the basis that left and right hemispheric structures have distinct roles in AM and episodic memory retrieval.[93,102,103,110,114,121,227]

Functional magnetic resonance pre-processing

MRI data were pre-processed using SPM12 (http://fil.ion.ucl.ac.uk/spm/). The first 5 volumes of each functional run were discarded to allow for T1 equilibration. Functional images were unwarped using the collected field maps[228] and slice-time corrected but left unsmoothed and in native space. Structural T1-weighted images were coregistered to the mean functional image of each participant. The structural image for each participant was segmented into gray matter, white matter, and cerebrospinal fluid using a nonlinear deformation field to map it onto a template tissue probability map.[229] Motion correction parameters estimated from the re-alignment

procedure and their first temporal derivatives (12 regressors in total) were included as confounds in the first-level analysis for each participant.

Representational similarity analysis

Representation Similarity Analysis (RSA) is a method used in multivariate pattern analysis (MVPA) to examine how similar or dissimilar the activity patterns are for the same versus different stimuli.[61,62] For each pair of trials, the multivariate distance (or similarity) between their activity patterns was measured using Pearson correlation. High similarity (high correlation or low distance; also denoted as low dissimilarity) indicates that the multivoxel patterns for the two trials are similar and may therefore involve the same set of neurons. Therefore, RSA provides an indirect measure of representational content within neuronal populations that is then associated with cognition. Unlike the standard mass-univariate analysis, which examines each voxel independently, RSA considers the joint activity of multiple voxels to decode information about experimental conditions. This allows for the detection of groups of voxels that represent very specific and subtle experimental conditions, such as specific episodic memories. There are several reasons for the high sensitivity afforded by MVPA: (1) RSA can combine weak but consistent signals from multiple voxels; distributed networks of very weakly active voxels that show no univariate effect may be detectable by RSA; and (2) it can measure the relationship between distal voxels where the relationship in their activity is required for memory representation, but the BOLD signal change might not be significant on univariate analysis.[14,42]

All RSAs were run on unsmoothed native-space functional images after the preprocessing steps described above had been completed. For each trial, a beta map was estimated using the general linear model (GLM) with maximum likelihood estimation implemented in SPM. We modeled two regressors of interest within our GLM trials: (1) the target trial of interest; and (2) all other trials, alongside other nuisance regressors. In this way, we generated one GLM per trial similar to a least squares single, so that we could better isolate the signal for each trial.[230] Each memory retrieval event was modeled separately from all other retrieval events both within runs and across runs. As memory retrieval events, including title screens, were 15s in duration and the TR for our EPI sequence was 3.36s, there were approximately four TRs per retrieval, but 67 TRs per memory condition (201 TRs for the episodic retrieval and control task conditions). The beta values were divided by the square root of the GLM residuals to reduce the impact of noisier voxels.[231] Resultant beta images were masked using a region of interest (ROI) approach, based on the network definitions listed above. Voxels with null values in any scan run were excluded. A split representational dissimilarity approach[14,231,232] was undertaken, with analyses conducted so that we computed retrieval-by-retrieval pattern similarity for each pair of trials (memory and counting, using trial-specific beta values) within runs and then these were averaged across the three runs. This split-RDM approach was employed to mitigate session-specific noise artifacts (e.g., scanner drift, physiological fluctuations) that can confound naturalistic autobiographical memory representations. This approach prioritised the assessment of within-run representational stability, our primary hypothesis concerning hippocampal function, while enabling us to avoid noise artifacts from extended acquisition times that would compromise cross-run comparisons.

Model matrix comparisons

We aimed to compare memory-by-memory correlations using two specific model hypothesis matrices to assess the following: (1) whether the observed hippocampal subfield pathology resulted in between-group differences in representational content during episodic memory retrieval, as a general process compared to the control task, across the network of ROIs (see Figure 4A); and, (2) whether hippocampal subfield pathology generated between-group differences in the capacity to represent specific episodic memories across the network of ROIs (see Figure 4B). Each run comprised 30 trials (15 trials per condition, with five trials per specific memory). Therefore, RDM model fit correlation scores were created from 465 within-run trial-by-trial correlation pairs (comparing each condition to all of the other trials per run), then averaged across runs. For the specific episodic memory retrieval hypothesis matrix, the counting trials were also modeled within the hypothesis matrix (creating a 30×30 matrix of trial-by-trial correlations), with the diagonal representing low dissimilarity. This is not shown in Figure 4B for simplicity. Model matrices were constructed to feature a value of 1 in hypothesised high-dissimilarity cells and a value of 0 in hypothesized low-dissimilarity cells. Beta images resulting from the preprocessing steps above, characterising the amplitude of the BOLD response to each trial, underwent pairwise comparisons to yield a Pearson Z dissimilarity score (computed as 1-Pearson correlation score) for each trial-by-trial comparison. Model fits were evaluated using a correlation between the pattern similarity matrix and the model matrices for each ROI, using Kendall τ (the memories were modeled as categorical data as well as being a smaller sample set; tested using a stimulus-label randomisation test by randomly permuting stimulus order for each subject 10,000 times to create a distribution of permuted within-subjects correlations under the null hypothesis that the hypothesis matrices could not be decoded, and thresholded to a false detection rate of $p < 0.05$). Model fits were then used in two separate ways: (1) to evaluate whether, for each group, the group level model fit was significantly different from the random condition using permutation testing, thereby suggesting the hypothesis matrix correctly modeled the multivoxel-patterned data; and, (2) as the basis to assess whether there was a between-group difference in degree of model fit, whereby we hypothesised that participants in the group with hippocampal amnesia would have significantly lower model fits within our ROIs. To our knowledge, there is no robust evidence to suggest that correlation values within different brain regions for the same task should be related, so between-group differences were assessed using between-group *t*-tests and orthogonality was assumed between the ROIs. Where a significant between-group difference was found for the specific episodic memory hypothesis matrix, we subjected the first-level Fisher-transformed Pearson scores for the individual memories (averaging the Fisher transformed Pearson

correlation scores for each pair of within-memory trials for the same within individual runs, and then across runs) to a 2 (group: group with hippocampal amnesia, controls) x 3 (experimental memories probed: 1, 2, and 3) omnibus ANOVA to assess whether any differences in model fit were represented in the first-level scores for that analysis.

We also sought to understand the relationship between these RSA results with the volumetric hippocampal subfield results and the internal (episodic) memory detail scores as detailed above using linear regression modeling, in line with our previous work.[31,37]

Statistical analyses

All t-tests, ANOVAs, linear regressions, and Sobel's test were performed on IBM SPSS Version 29.0 (IBM Corp.).